Design, Synthesis, and Biological Evaluation of Potent and Selective Class IIa Histone Deacetylase (HDAC) Inhibitors as a Potential Therapy for Huntington's Disease

Roland W. Bürli,[†] Christopher A. Luckhurst,[†] Omar Aziz,[†] Kim L. Matthews,[†] Dawn Yates,[†] Kathy. A. Lyons,[‖] Maria Beconi,[§] George McAllister,[†] Perla Breccia,[†] Andrew J. Stott,[†] Stephen D. Penrose,[†] Michael Wall,[†] Marieke Lamers,[†] Philip Leonard,[†] Ilka Müller,[†] Christine M. Richardson,[†] Rebecca Jarvis,[†] Liz Stones,[†] Samantha Hughes,[†] Grant Wishart,[†] Alan F. Haughan,[†] Catherine O'Connell,[†] Tania Mead,[†] Hannah McNeil,[†] Julie Vann,[†] John Mangette,[‡] Michel Maillard,[§] Vahri Beaumont,[§] Ignacio Munoz-Sanjuan,[§] and Celia Dominguez*,[§]

[†]BioFocus, Chesterford Research Park, Saffron Walden, Essex, CB10 1XL, United Kingdom
[‡]AMRI, Inc., 26 Corporate Circle, Albany, New York 12212, United States
[§]CHDI Management/CHDI Foundation Inc., 6080 Center Drive, Suite 100, Los Angeles, California 90045, United States

S *Supporting Information*
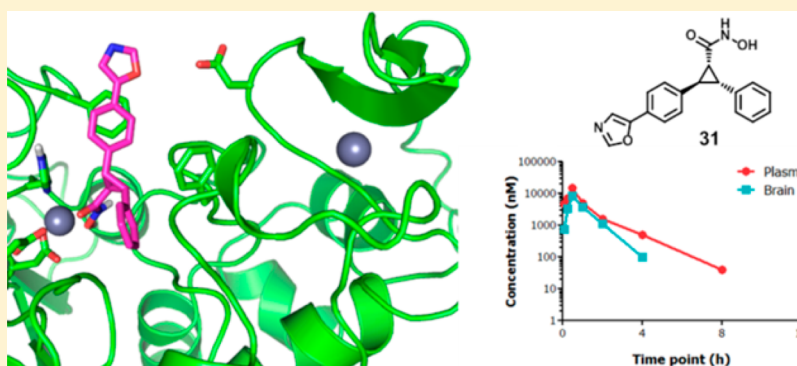
ABSTRACT: Inhibition of class IIa histone deacetylase (HDAC) enzymes have been suggested as a therapeutic strategy for a number of diseases, including Huntington's disease. Catalytic-site small molecule inhibitors of the class IIa HDAC4, -5, -7, and -9 were developed. These trisubstituted diarylcyclopropanehydroxamic acids were designed to exploit a lower pocket that is characteristic for the class IIa HDACs, not present in other HDAC classes. Selected inhibitors were cocrystallized with the catalytic domain of human HDAC4. We describe the first HDAC4 catalytic domain crystal structure in a "closed-loop" form, which in our view represents the biologically relevant conformation. We have demonstrated that these molecules can differentiate class IIa HDACs from class I and class IIb subtypes. They exhibited pharmacokinetic properties that should enable the assessment of their therapeutic benefit in both peripheral and CNS disorders. These selective inhibitors provide a means for evaluating potential efficacy in preclinical models in vivo.

INTRODUCTION

The histone deacetylase (HDAC) superfamily consists of 18 members (HDACs 1−11 and the class III sirtuins 1−7) originating from two different evolutionary starting points, which exhibit a common deacetylase activity of acetylated ε-amino groups of lysine side chains. In addition to deacetylation of histones, these enzymes act on numerous proteins, the so-called lysine '"acetylome",[1] and they have been implicated in a diverse array of biological pathways governing transcriptional and epigenetic control, cell differentiation and cell death, cardiac function, inflammation, protein proteostatis, and neuroplasticity, often as part of complexes with other proteins (extensively reviewed).[2−5]

The "classical" HDAC family consists of 11 zinc-dependent HDACs that are grouped into three classes (classes I, II, and IV). Class I members (HDACs 1−3, 8) as well as the class IV enzyme, HDAC11, contain an N-terminal catalytic domain that constitutes most of their ∼440 amino acid length, contain nuclear localization motifs (HDACs 1, 3 and 8), or lack nuclear export signals (HDACs 1 and 2), allowing them to reside either preferentially or exclusively in the nucleus (except HDAC3, which contains both nuclear import and nuclear export sequences). The class I enzymes are the "prototypical enzymes"
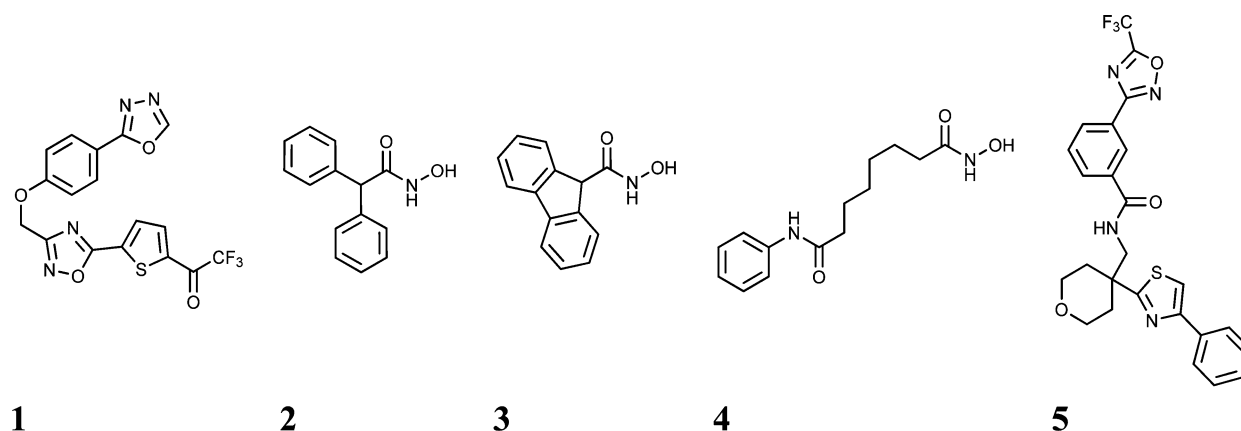
Figure 1. Structures of selected literature compounds.

in that they display very efficient histone deacetylation activity; however, HDAC8 is atypical and resembles a class IIa enzyme in substrate recognition.[6]

Class II HDACs are subdivided into class IIa (HDACs 4, 5, 7, 9) and class IIb (HDACs 6, 10) enzymes. The class IIb enzymes are catalytically avid, similar to class I enzymes, but are characterized by two catalytic domains and a cytoplasmic location; however, only in HDAC6 are the two domains functional.[7]

The class IIa members are about 1000 amino acids in length and are exemplified by the presence of a well-conserved extended N-terminus containing multiple transcription factor binding sites that are important for the regulatory function of these proteins.[8] These enzymes reside in both the cytoplasm and nucleus, and cellular trafficking of these HDACs is regulated by intrinsic nuclear import and export signals as well as binding sites for 14-3-3 proteins. Binding to the 14-3-3 proteins stimulates the cytoplasmic retention or nuclear export of the class IIa HDACs in a phosphorylation-dependent manner of which multiple kinase signaling pathways have been implicated. This regulation of subcellular location in turn regulates the transcriptional activity of the class IIa enzymes by limiting accessibility to their nuclear transcription partners, including members of the MEF2 family.[8,9] Compared to the class I HDACs, the catalytic deacetylation activity of all class IIa enzymes is intrinsically much weaker (∼1000-fold lower) because of a Tyr to His switch in the active site. No natural substrate of class IIa enzymes has been conclusively identified that can be ascribed purely to the catalytic activity of the enzyme rather than its class I/III HDAC binding partners.[6,10,11] This questions the class IIa HDACs' bona fide deacetylase activity; the "catalytic domain" may serve instead as a recognition domain for binding to N^ε-acetyllysine residues of proteins to orchestrate protein−protein interactions and macromolecular protein signaling.[12,13]

Class IIa HDACs have been implicated as potential targets for the treatment of a number of diseases. The role and potential benefit of HDACs 4, 5, 7, and 9 "inhibition" in a number of cancers are comprehensively reviewed elsewhere.[9] Class IIa enzymes have also been suggested as viable drug targets for various metabolic disorders, including type II diabetes, owing to their regulation of glucose homeostasis and muscle glucose metabolism.[14,15] Class IIa enzyme inhibition has also been proposed for the treatment of pathological cardiac hypertrophy,[3,16−22] acute ischemic injury (HDAC4),[23] and inflammatory or autoimmune conditions,[24]

such as the pathophysiology of colitis (HDAC9)[25] and liver disease.[26]

A particular interest of our group is in the role of HDAC4 in Huntington's disease.[27] When HDAC4 heterozygous knockout animals were crossed with the R6/2 mouse model of Huntington's disease (HD), it led to significant improvement in motor coordination and neurological phenotypes, improved medium spiny neuron properties and corticostriatal synaptic function, and increased R6/2 lifespan.[28] Furthermore, HDAC4 reduction delayed cytoplasmic aggregate formation in both R6/2 and the full length mHtt Q150 knock-in mouse model.[28] Class IIa HDACs have also been implicated in the etiology of other CNS disorders, such as Alzheimers disease[29] and mood disorders[30−34] and perhaps most prominently in their potential as treatment for muscle wasting disorders and motor neurone diseases. HDAC4 in particular has been strongly implicated in controlling muscle differentiation and neuromuscular homeostasis through a nuclear MEF2-dependent process that relies predominantly on CamKII regulation of subcellular enzyme location.[35,36] The expression of HDAC4 appears to be highly controlled in muscle by specific microRNAs,[37,38] contributing to the tight regulation of muscle differentiation. HDAC4 is robustly induced in either acutely denervated muscles or those affected by motor neuron diseases such as amyotrophic lateral sclerosis (ALS). Muscle atrophy represents a rare instance where the published biology supports a specific and essential role for the catalytic domain of HDAC4.[39]

In most of the biological studies cited here, the suggestion for the potential therapeutic benefit from class IIa HDAC inhibition has arisen either from genetic suppression studies of various class IIa isoforms or from a combination of genetic evidence indicating class IIa enzyme involvement with additional efficacy achieved with broad spectrum HDAC inhibitors. Because of the unique nature of the class IIa enzymes, namely, the regulatory role of the extended N-terminal domain interactions and the weak deacetylase activity, a critical issue is whether or not occupancy of the class IIa catalytic domain with small molecules will be capable of replicating, either fully or in part, the beneficial effects of class IIa HDAC knockdown proven to be efficacious in various preclinical paradigms. The work described here on the development of novel selective class IIa inhibitors with potent cellular activity and improved pharmacokinetic properties sufficient to evaluate their therapeutic benefit in vitro and in vivo will help greatly to address these questions. Given our particular interest in HDAC4 inhibition (for the treatment of

Table 1. Biochemical and Cell-Based IC$_{50}$ Values for Reported Trifluoromethyl Ketones, Hydroxamic Acids, and SAHA

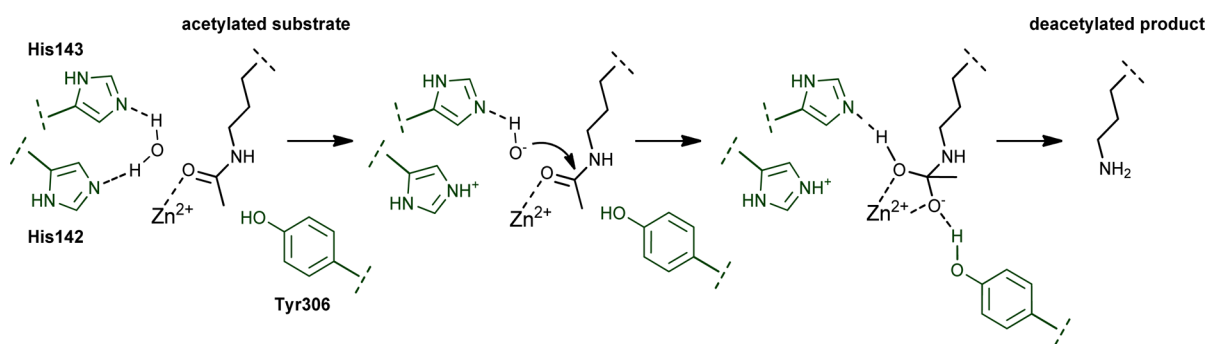|	HDAC4 (μM)	HDAC5 (μM)	HDAC7 (μM)	HDAC9 (μM)	HDAC3 (μM)	HDAC6 (μM)	HDAC8 (μM)	cell activity Lys-TFA (μM)	Lys-Ac (μM)	AlogP	tPSA (Å^2)	M_w
1	0.01	0.01	0.07	0.02	0.38	0.28	0.22	0.26	0.85	3.5	104	422
2	0.25	0.16	0.65	0.51	>50	11	45	2.9	>50	2.4	49	227
3	0.31	0.15	0.07	0.12	39	4.9	15	0.97	>50	2.1	49	225
4	41	4.6	41	49	0.25	0.03	0.64	>10	0.04	2.0	78	264
5[a]	0.13	0.08	0.04	0.02	>43	2.3	3.6			4.3	90	514

[a]Literature data.

Figure 2. Schematic presentation of the deacetylase mechanism of class I HDACs. Key residues of class I HDAC protein are in green, and numbering of residues is according to HDAC8. The position of Tyr306 in the class I HDAC subtypes overlaps with His976 (HDAC4 numbering) in the class IIa subtypes. The His residue can rotate away from the Zn^{2+} ion, opening up the lower pocket.

Huntington's disease), we have focused our medicinal chemistry strategy on this enzyme as representative of the class IIa isoforms.[40]

RESULTS AND DISCUSSION

In order to assess the efficacy of compounds against HDAC activity, a selection of biochemical assays were performed as described previously.[41] Compound potency against the following HDACs was interrogated either as full length proteins (HDAC1, HDAC2, HDAC3-NCoR2, HDAC6, HDAC8) or as catalytic site truncated proteins expressed recombinantly (HDAC4, HDAC5, HDAC7, and HDAC9).

Cellular assays employed artificial substrates Boc-Lys(Ac)-AMC[42,43] and Boc-Lys(TFA)-AMC[10,44] in Jurkat E6.1 cells using endogenous HDAC activities, as described previously.[41] Utilizing gene selective shRNAs, class IIa HDACs were knocked-down individually and collectively in Jurkat E6.1 cells to demonstrate that the majority of class IIa HDAC activity in this cell line is derived from HDAC4 (Supporting Information).

At the outset of this project, two structural types of selective class IIa HDAC inhibitors had been reported: trifluoromethyl ketones and hydroxamic acids (selected examples are shown in Figure 1).[45−51] In order to understand which chemotype may serve as a suitable starting point for the development of a tool molecule, we evaluated key representatives of each series and compared them to SAHA (4, Table 1). During the preparation of this manuscript structures of trifluoromethyloxadiazole class IIa inhibitors were disclosed (5, Table 1).[52] SAHA was found to be a potent inhibitor of class I isoforms (HDAC1, 0.03 μM; HDAC2, 0.92 μM; HDAC3, 0.25 μM; HDAC8, 0.64 μM) and class IIb (HDAC6, 0.03 μM) in biochemical assays, with relatively weak inhibitory activity for the class IIa isoforms. This observation was further confirmed by the difference in activity in the Lys-Ac "class I/IIb-specific" versus the Lys-TFA "class

IIa/HDAC8-specific" cell-based assays, in which the conversion of either a Boc-Lys-Ac (Ac) or a Boc-Lys-TFA (TFA) substrate was monitored.[12,41] When compared to SAHA, all four reference compounds (1−3) demonstrated a very different selectivity profile and were more potent inhibitors for the class IIa isoforms. The hydroxamic acids (2 and 3), although less potent HDAC4 inhibitors, generally showed a lower shift in potency from biochemical to cellular activity (TFA) and did not show significant activity up to 50 μM under the "class I/IIb-specific" assay conditions.

Trifluoromethyl ketones are intrinsically electrophilic,[19] whereas hydroxamic acids have successfully been progressed to proof-of-concept studies preclinically and in humans for other indications.[53] We reasoned that optimization of HDAC4 inhibitors bearing a hydroxamic acid metal binding group would provide a rapid avenue toward a molecule suitable for a proof-of-concept study.

To understand the binding mode of these ligands, publicly available structural data across the HDAC family, along with mutation data and SAR for HDAC4, were analyzed.[45−47] Most relevant to this work, Bottomley et al. published two structures of the catalytic domain complexed with a trifluoromethyl ketone and an analogous hydroxamic acid.[45,54] A comparison of these structures with the previously reported HDAC8 substrate−mimetic complex revealed the existence of a lower pocket in HDAC4.[55] This is formed by replacement of a tyrosine residue by a histidine (His976 in HDAC4), which rotates away from the binding site. This Tyr to His switch is highly conserved and characteristic for the class IIa enzymes and accounts for their decreased deacetylation activity.[45] The HDAC4 lower pocket therefore appears to be specific for the class IIa HDAC family and was envisaged to provide an opportunity to pursue selectivity. Furthermore the HDAC4 lower pocket differs from the previously described HDAC2 foot pocket.[56] For HDAC4 the backbone path between residues
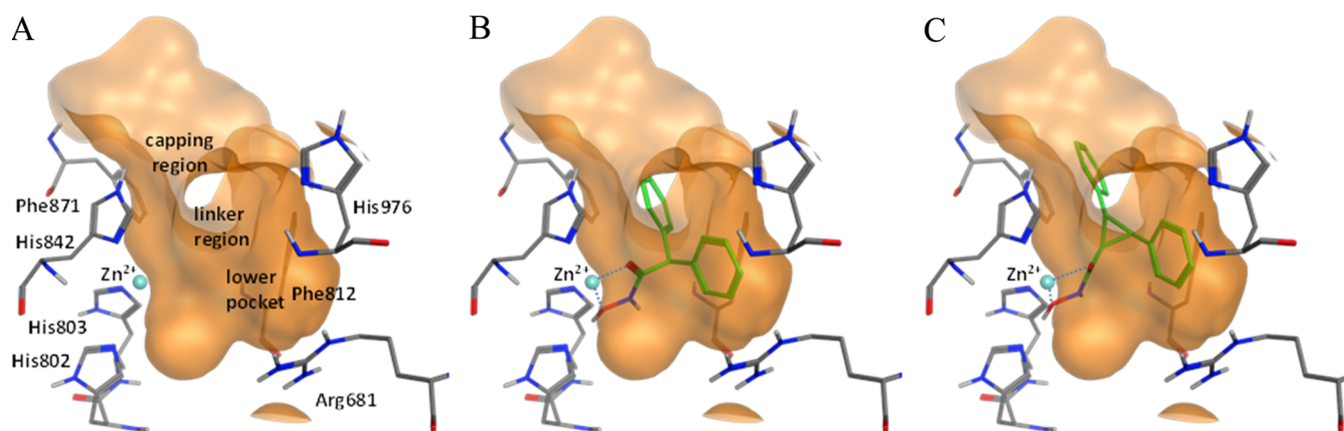
Figure 3. Modeled representation of the HDAC4 active site: (A) HDAC4 active site illustrating the zinc binding region, the lower selectivity pocket, and a channel bounded by Phe871 and Phe812; (B) docked compound **2** showing occupation of the lower pocket, the linker region, and zinc interactions; (C) docked compound (2R,3R)-**15** showing occupation of the lower pocket, the linker region, and zinc interactions.

Table 2. Activity of the First Di- and Trisubstituted Cyclopropanes[a]

		(rac)-**15**	**16**	(rac)-**17**	(rac)-**18**
HDAC4	(μM)	0.34	>50	51	904
Lys-TFA	(μM)	2.52	>50	>50	>50
Lys-Ac	(μM)	>50	>50	>50	>50

[a]HDAC4 biochemical and cell data (Lys-TFA and Lys-Ac) are shown. Compound syntheses are described in the Supporting Information.

Gly797 and Gly801 deviates from that of HDAC2, resulting in the placement of HDAC4 residue Pro800 into the previously described foot pocket region. Therefore, the HDAC2 foot pocket is not present in the disclosed structures of HDAC4.

Figure 2 illustrates the proposed deacetylase mechanism of class I, IIb, and IV HDAC families, in which a Tyr participates in the catalytic event.

The known HDAC7/SAHA and trichostatin A (TSA) bound structures also indicated the presence of a similar lower pocket.[57] We hypothesized that this pocket could be exploited to obtain selectivity over the class I and class IIb HDAC isoforms.

Sequence analysis revealed that the class IIa HDAC isotypes are highly homologous around the catalytic deacetylation site (described in Supporting Information). It is therefore not surprising that the HDAC4 inhibitors (**1**−**4**) displayed very similar activity across all class IIa isotypes (Table 1). On the basis of this high degree of similarity within the catalytic site, we anticipated difficulty in rationally designing HDAC4 inhibitors with a pharmacologically relevant degree of selectivity over the other class IIa isoforms.

Contrary to most HDAC structures, the loop regions between residues Glu24 and Arg37 as well as Thr81 and Ala126 (numbering based on published data)[45] of the reported HDAC4 (catalytic domain) structure adopted an open conformation. Mutation data suggest that a loop-closed form is necessary for enzymatic activity.[45,58,18,26] We developed an HDAC4 model in which this loop resides in a closed conformation. On the basis of the docking result with

compound **2** (Figure 3), we envisaged that a trisubstituted cyclopropane core may provide a scaffold with suitable vectors to occupy the catalytic site. Initial docking of N-hydroxy-2,3-diphenylcyclopropanecarboxamide showed that the trans-(2R,3R)-cyclopropane isomer (single enantiomer of compound **15** in Table 2) positioned the hydroxamic acid function next to the zinc(II) cation and one phenyl in the lower pocket while directing the second phenyl group toward a hydrophobic channel or linker region (Figure 3). It was reasoned that the second phenyl group may be further substituted with functionalities capable of projecting toward the solvent space (capping region). Conversely, docking of the diastereomer cis-(1r,2S,3R)-**16** (Table 2) predicted that the configuration of this compound precluded occupancy of both the lower pocket and linker regions by the phenyl groups.

Chemistry. Synthetic access to these cyclopropane scaffolds proved to be challenging. Our initial attempts to cyclopropanate styrenes with a metallocarbenoid were at best very low yielding. However, we identified suitable conditions using a sulfur ylide-mediated cyclization to facilitate the key synthetic step in accessing a trisubstituted cyclopropane scaffold.[59−61] To the best of our knowledge, this is the first reported example of a semistabilized sulfur ylide reacting with a cinnamic ester leading to a 1,2,3-substituted cyclopropane core. Treatment of the esters **6a**−**c** with the corresponding sulfur ylide gave rise to the cyclopropane esters **7a**−**c** as mixtures of diastereoisomers. Notably, addition of 12-crown-4 ether improved the diastereoselectivity in favor of the desired trans isomer (1R*,2R*,3R*) over the cis form (1R*,2S*,3R*) (Scheme 1), providing a 1:1

Scheme 1. Synthesis of Phenyl-Linked Cyclopropanes[a]

6a,7a: R[1] = Et, R[2] = Br, R[3] = H
6b,7b: R[1] = Me, R[2] = H, R[3] = Br
6c,7c: R[1] = Et, R[2] = F, R[3] = Br
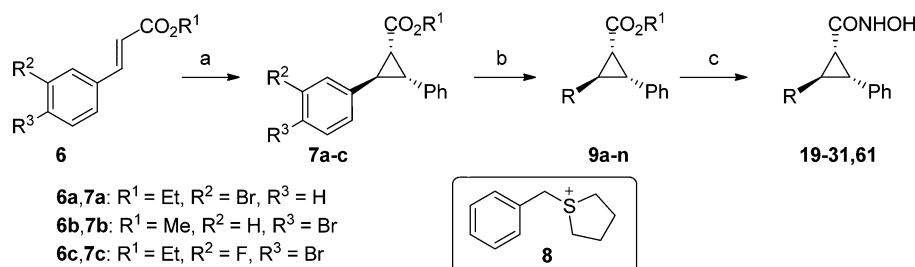
[a]Reagents and conditions: (a) **8** (OTf or Br salt), LiHMDS, 12-crown-4, −20 °C, 2 h, 25%. (b) For **9a−c**: amine, Pd$_2$(dba)$_3$, xantphos, Cs$_2$CO$_3$, dioxane, 90 °C, 16 h, 59−82%. For **9e** and **9k**: boronic acid, Pd(PPh$_3$)$_4$, CsF, MeOH−DME (1:5), 120 °C microwave, 1 h, 93%. For **9d** and **9f−h**: (Bpin)$_2$, Pd(dppf)Cl$_2$, KOAc, 100 °C, 2 h, then R-X, Pd(PPh$_3$)$_4$, Na$_2$CO$_3$, 100 °C, 2 h, 46−100%. For **9i**, **9j**, **9l**: stannane, Pd(PPh$_3$)$_4$, dioxane, 150 °C microwave, 1 h, 73−84%. For **9m−n**: oxazole, Pd(OAc)$_2$, tetramethyl-di-^{t}BuXPhos, K$_2$CO$_3$, pivalic acid, DMA, 110 °C for 16 h, 65−100%. (c) NH$_2$OH, KOH, MeOH−THF (1:1), rt, 1 h, 65−100%.

trans/cis ratio instead of the 1:2.5 ratio obtained without additive. Palladium-catalyzed coupling reactions under Heck, Suzuki, or Stille conditions installed the capping group and provided ester intermediates **9a−n**, which were converted to their corresponding hydroxamic acids.

Similarly, final compounds **32−60** were obtained from their corresponding α,β-unsaturated esters (Scheme 2). The starting

Scheme 2. Synthesis of Bicyclic and Heterocyclic Compounds (32−60)[a]
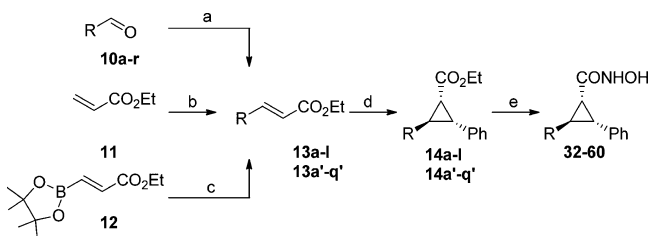
[a]Reagents and conditions: (a) (EtO)$_2$P(O)CH$_2$CO$_2$Et, NaH, THF, 0 °C to rt, 1 h, 44−99%; (b) RCl or RBr, Pd(OAc)$_2$, P(o-tol)$_3$, NEt$_3$, MeCN, 80 °C, 3−18 h, 17−93%; (c) RBr, Pd(PPh$_3$)$_4$, K$_2$CO$_3$, dioxane, 100 °C, 17 h, 68%; (d) **8** (OTf or Br salt), LiHMDS, 12-crown-4, −20 °C, 2 h, 16−100% (dr > 98:2 to 5:4); (e) NH$_2$OH, KOH, MeOH−THF (1:1), rt, 1 h, 5−86%.

enoates (**13**) were synthesized either via Heck, Wittig, or Suzuki reactions from the corresponding aldehydes or bromides. The identity and purity of all final molecules were determined by ^{1}H NMR, mass spectrometry, and analytical HPLC. Purities were in excess of 95%. Separation of enantiomers was achieved for selected compounds using HPLC and a chiral stationary phase (Supporting Information). The enantiomeric excess values for the compounds described herein all exceeded 95%.

Structure−Activity Relationships. The trisubstituted cyclopropane **15**, in which the two phenyl groups are in trans-configuration relative to each other, displayed submicromolar inhibitory activity for HDAC4 in the biochemical assay and low micromolar activity in the cellular context (Table 2). In contrast, its diastereomer **16** showed no significant HDAC4 inhibition and validated our modeling hypothesis described earlier. The biochemical activity of the two disubstituted diastereomers (**17**, **18**) differed by about an order of magnitude. Modeling suggested that the phenyl group of the cis fragment **17** fills the lower pocket, whereas the phenyl unit

of the trans diasteromer **18** points toward the hydrophobic channel (later confirmed by X-ray of close analogues; vide infra). These observations highlighted the large gain in affinity upon engagement of the lower pocket, and initial cell potency data confirmed the predicted selectivity over the class I isoforms.

The capping group was investigated with the objective of improving potency while achieving balanced physicochemical properties suitable to achieve CNS exposure. Accordingly, we aimed for molecules with AlogP values ranging from 2 to 4, a polar surface area below 80 Å^2, and a limit of two hydrogen bond donor functions. Simple heterocycloalkyl capping groups showed no improvement in potency as illustrated by the activity of racemic, cyclic anilines **19**, **20**, and **21**, respectively (Table 3). An improvement in both biochemical and cell-based potency was observed following para-substitution of the phenylene linker with heteroaryl capping groups; for instance, pyridazine **22** and pyrimidines **23** and **24** (with AlogP values between 2 and 3) displayed HDAC4 inhibitory activity below 100 nM.

The high ligand efficiency (LE = 0.4)[62] and ligand lipophilicity efficiency (LLE = 4.9)[63] observed for **24** warranted further exploration of the general phenyl linker-capping heterocycle architecture (Table 3). The 4-fluoro-substituted analogue (*R,R,R*)-**25** demonstrated a cellular potency of roughly 300 nM in the "Lys-TFA" assay, while no significant inhibition was detected under "Lys-Ac" conditions (up to 50 µM). Compound **25** was among the analogues with higher passive permeability in Madin−Darby canine kidney (MDCK) cells ($P_{appA \rightarrow B}$ = 294 nm/s) and was not a substrate of P-gp in vitro as determined by an effective efflux ratio (EER) of 1.4 in MDCK-MDR1 cell monolayers. Hydroxamic acids are known to be glucuronidated and metabolized by aldehyde oxidase;[64−66] the fractional contribution of these processes to the in vivo clearance is difficult to predict from in vitro systems. Hydroxamic acids can also undergo CYP metabolism; thus, our first objective was to minimize the potential for oxidative metabolism, and hence, we evaluated the stability of the compounds in liver microsomes. Compound **25** had relatively poor metabolic stability in MLM (Cl$_{int}$ = 688 mL min^{-1} kg^{-1}) but acceptable stability in HLM (Cl$_{int}$ = 42 mL min^{-1} kg^{-1}). We reasoned that while increasing the number of heteroatoms may reduce metabolic liability, escalating polar surface area would lead to reduced distribution to brain tissue.

Given the encouraging potency and properties observed with the pyrimidin-2-yl capping group, additional polar azole

Table 3. Biological, in Vitro ADME Data and Selected Calculated Properties for Phenylene Linker Scaffold with Varying Capping Group Substituents[a]

	R	cat. HDAC4 (μM)	cell-based activity (μM)		microsomal stability Cl_{int} (mL/min/kg)		MDCK-MDR1 (ratio; nm/s)		AlogP TPSA (Å^2) M_w
			Lys-TFA	Lys-Ac	MLM	HLM	EER	$P_{app\ A\rightarrow B}$	
(rac)-19		0.33	3.2	>50	>1297	<40	-	-	3.4 53 336
(rac)-20		0.15	1.3	>50	-	-	-	-	2.0 62 350
(rac)-21		0.15	1.8	>50	-	-	-	-	3.2 53 358
(rac)-22		0.08	0.62	>50	323	<36	-	-	2.8 75 331
(rac)-23		0.10	1.2	>50	124	49	4.2	351	2.3 75 331
(rac)-24		0.06	0.62	>50	>1297	<36	-	-	2.4 75 331
25		0.05	0.31	>50	688	<42	1.4	294	2.6 75 349
(rac)-26		0.10	1.0	>50	95	<36	-	-	2.6 75 349
(rac)-27		0.29	2.0	>50	380	<36	-	-	2.5 67 333
(rac)-28		0.10	0.46	>50	74	47	1.1	10	2.5 78 333
29		0.06	0.40	>50	476	-	8.2	110	2.7 78 351
(rac)-30		0.05	0.35	>50	>1297	<38	-	-	2.3 76 320
31		0.02	0.22	>50	89	<36	2.4	442	2.2 76 320

[a]Generic structure shown in Scheme 1. Intrinsic clearance (Cl_{int}) values of >257 mL min^{-1} kg^{-1} in mouse liver microsomes and >52 mL min^{-1} kg^{-1} for human liver microsomes indicate a rapid rate of oxidative metabolism. Under the assay conditions used Cl_{int} values of <65 mL min^{-1} kg^{-1} in MLM and <36 mL min^{-1} kg^{-1} in HLM indicate low rate of metabolism by CYP450 enzymes. An effective efflux ratio (EER) value of >4 predicts that a compound is a substrate for P-gp, whereas values of <2 suggest the compound is not a P-gp substrate.

substitution patterns were explored (Table 3). N-Methylimidazole 27 displayed a loss in potency against HDAC4 (0.29 μM), indicating that ortho-substitution on the capping group was deleterious, likely because of a twist of the capping group and loss of biaryl planarity. Transfer of the methyl group to the adjacent carbon heterocyclic position (28) improved biochemical and cellular activity by 3- to 5-fold. This NH-imidazole was relatively stable in MLM (Cl_{int} = 74 mL min^{-1} kg^{-1}); however, introduction of the additional H-bond donor function reduced its passive permeability ($P_{appA\rightarrow B}$ = 10 nm/s) and is therefore likely to have reduced oral exposure and CNS access compared to other compounds in the series. In an attempt to mitigate this, a fluorine atom was incorporated on

the adjacent phenyl linker of compound 29. It was anticipated that this modification would shield the NH function of the imidazole element. Indeed, the fluoro analogue 29 demonstrated a 10-fold increase in passive permeability relative to 28 but showed high P-gp-mediated efflux (EER = 8.2) and was metabolically unstable (MLM Cl_{int} = 476 mL min^{-1} kg^{-1}).

Oxazole capping groups were investigated with the objective of exploiting a pharmacophore similar to the imidazoles described above, with removal of the extra hydrogen bond donor (Table 3). The 2-substituted oxazole (rac)-30 was potent under biochemical and cellular conditions but displayed high intrinsic clearance in mouse liver microsomes, likely because of the exposure of the oxazole C(4)−H and C(5)−H.

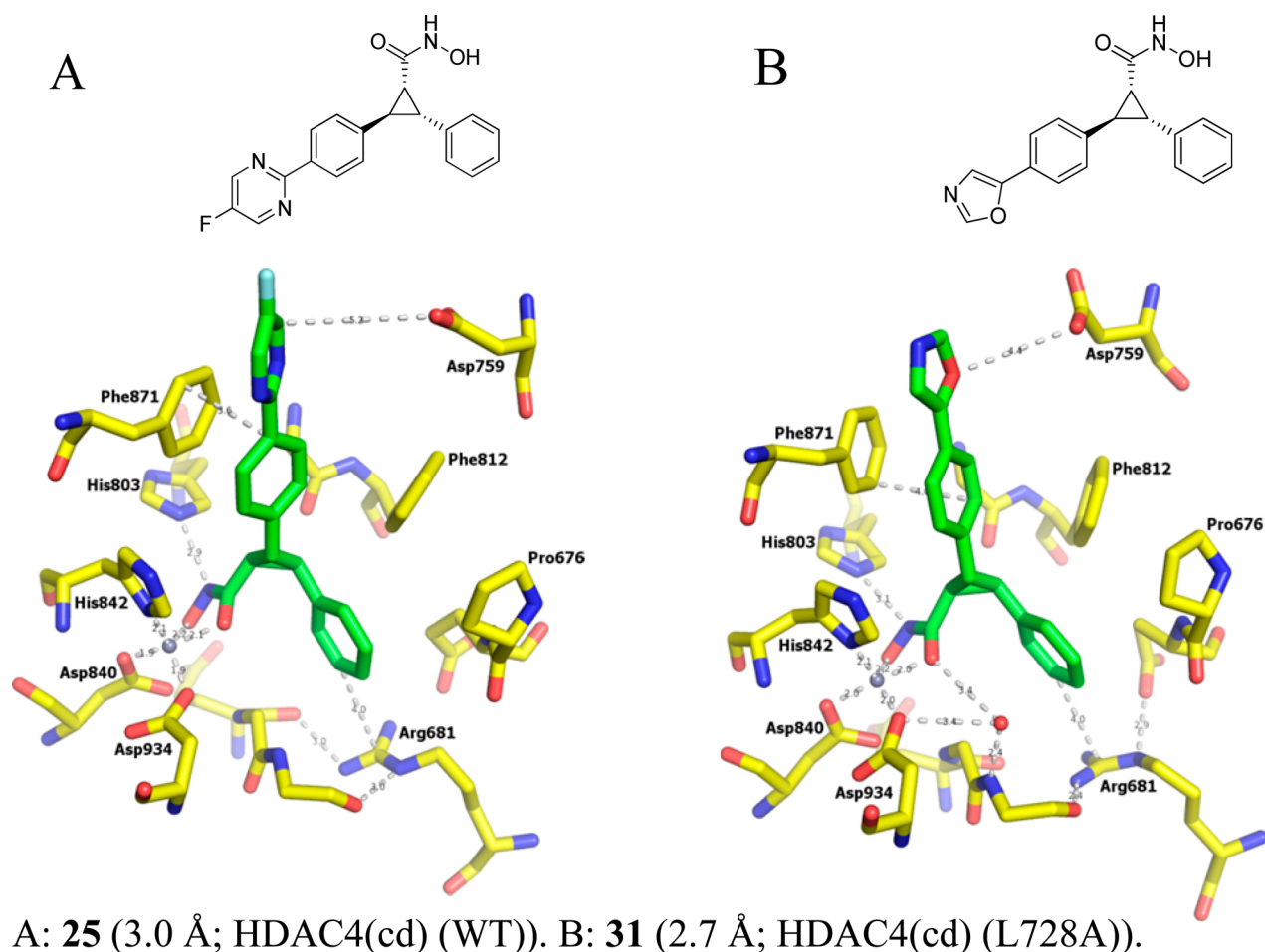A: **25** (3.0 Å; HDAC4(cd) (WT)). B: **31** (2.7 Å; HDAC4(cd) (L728A)).

Figure 4. HDAC4 cocrystal X-ray structures.

However, the 5-substituted regioisomer **31** was relatively stable in liver microsomes and had the highest passive permeability of all the analogues evaluated. It also exhibited slightly improved potency (HDAC4, 25 nM; cell, 220 nM), excellent ligand efficiency (LE = 0.43; LLE = 5.4), and effective efflux ratio (EER) of 2.4. It was progressed to in vivo pharmacokinetic studies (PK discussed in pharmacokinetic studies section). Compound **31** was found to be a potent inhibitor of human hepatic CYP450 isoforms CYP2C9 (IC$_{50}$ ≈ 0.4 μM) and CYP2C19 (IC$_{50}$ ≈ 0.06 μM) and a moderate inhibitor of CYP2D6 (IC$_{50}$ ≈ 2.7 μM), which was attributed to the C(2) unsubstituted oxazole moiety. While further work with oxazole capping groups to address the CYP450 inhibition was undertaken (discussed later), this was not a concern for moving compounds forward to nonclinical PoC.

In order to determine the configuration of active cyclopropane inhibitors and their key interactions with HDAC4, we obtained a cocrystal structure of 5-fluoropyrimidine **25** complexed to the catalytic domain of wild type human HDAC4 (Figure 4A). This structure crystallized in the space group $P3_2$ with three molecules per asymmetric unit (data not shown). In contrast to the previously reported HDAC4 structures,[45] the protein adopts a closed-loop conformation, which is consistent with the previously documented structures for HDAC7 and HDAC8.[57,58] Inspection of the crystal packing in the complex between HDAC4 and **25** showed that the ligand binding site forms part of a packing interface in which residue Leu728 of a neighboring HDAC4 chain is positioned close to

the ligand and has the potential to affect the bound compound conformation. In addition, it was observed that amino acids 729 to 760 were not visible in the electron density maps for any of the three molecules in the asymmetric unit and were omitted from the model because of disorder. As a result, we could not study the interaction between the ligand and key residue Asp759, a mutation to alanine that has previously resulted in a significant loss of deacetylase activity.[67]

In order to improve crystal packing and avoid the potential interference of Leu728 as described above, we mutated this residue to a sterically less bulky alanine. Indeed, HDAC4(cd) (L728A) yielded cocrystal structures with several ligands, including lead molecule **31** (Figure 4B) in a novel crystal form. The complex with **31** has been solved at 2.72 Å resolution and contains four protein molecules per asymmetric unit. Importantly, no crystal packing contacts were observed near the ligand binding site, and the loop between residues 727 and 761, which forms the rim of the binding site, was resolved in this structure. Activity of the L728A mutant of the HDAC4 catalytic domain was assessed in an identical manner as that of the wt HDAC4 catalytic domain, with activity compared at equal amounts of protein for both enzymes (0.2 μg/mL) and using the same substrate (Boc-Lys(TFA)-AMC) (data not shown). Higher concentrations of the L728A mutant clearly demonstrate that the activity scales well with increasing concentration and that this activity was inhibited to the same extent using a reference compound, when compared to wt HDAC4. These data demonstrate not only that the L728A

mutant HDAC4 catalytic domain protein is active but also that the extent of the activity was identical to that of the wt HDAC4 catalytic domain protein using the assays detailed.

The cocrystal structure of the 5-fluoropyrimidine **25** with HDAC4(cd) (WT) allowed the unambiguous assignment of the absolute configuration of this ligand and confirmed the binding pose as anticipated from docking studies (Figure 4A). A detailed analysis of the crystal structure showed that the hydroxamic acid moiety forms a bidentate interaction with the zinc(II) ion, with the carbonyl and the hydroxy oxygen atoms located 2.00 and 2.36 Å apart from the metal ion. This chelation completes the coordination sphere for the zinc ion, which includes a carboxylate oxygen atom of Asp840, one interaction from a His842 ring nitrogen, and one contact from Asp934 (Figure 4A). The hydroxamate OH group of **25** also serves as a hydrogen bond donor to His802 with a distance of 2.36 Å between heavy atoms. While the distance (2.97 Å) and angle are not ideal, an interaction may be postulated between His803 and the hydroxamic acid NH. The lower pocket, as anticipated, is formed by His976 oriented away from the metal ion and is occupied by the ligand's phenyl group, which undergoes favorable edge-to-face π-stacking interactions with Arg681 and Phe812. In addition, a number of lipophilic interactions were observed, for example, to Pro676, Pro800, and Leu943. The ligand linker region occupies a hydrophobic channel, bordered by Gly811, Phe812, His842, Pro942, Leu943, and Phe871. Phe871 forms a face−face π-stacking interaction with the linker phenyl ring, while the terminal pyrimidine cap extends toward solvent. Apart from a van der Waals contact with Pro942 (4.36 Å), no interactions with the capping group were observed.

The crystal structure of oxazole **31** complexed with the HDAC4(cd) (L728A) (Figure 4B) is consistent with the **25** HDAC4(cd) (WT) structure (Figure 4A); a minor change in the His803 conformation appeared to improve the hydrogen bonding between this residue and the NH of the hydroxamic acid functionality. Interestingly, the loop region bearing Asp759 is more ordered in this structure and no direct interaction between Asp759 and the ligand was observed.

To confirm the importance of an aromatic linker π-stacking interaction with Phe871 in the HDAC4 binding site, the phenyl ring was replaced by a cyclopentane in **32** (Table 4). This led to a 25-fold drop in HDAC4 biochemical potency, likely due to the absence of this interaction.

From the X-ray structural information of compounds **25** and **31**, it appeared that there were no direct interactions between the capping group heterocycles and the protein residues. This encouraged the design and synthesis of lower molecular weight molecules bearing small aliphatic substituents. It was envisaged that the desirable physicochemical properties that had been conferred by the polar capping groups with the phenyl linker could be attained with a heterocyclic linker in its own right. Accordingly, a series of heteroaromatic linker scaffolds were evaluated (Table 4).

Compounds comprising azole linkers were synthesized and profiled. The N-methylpyrazole **33** and thiazole **34** displayed only moderate HDAC4 activity. The 2-methyl-5-thiazole **35** was roughly 5-fold more potent in the biochemical assay, although all three compounds showed cellular activity in the low micromolar range. We therefore concluded that a heteroatom in proximity to the cyclopropane core may be detrimental for HDAC4 activity. Nevertheless, these compounds displayed high ligand efficiencies and ligand-lip-

Table 4. Structure−Activity Data for Cyclopentane and Heteroaromatic Linkers with Small Substituents[a]

	R	cat. HDAC4 (μM)	cell-based activity (μM)		AlogP TPSA (Å²) M$_w$
			Lys-TFA	Lys-Ac	
(rac)-**32**	(structure)	9.0	48	>50	2.7 49 245
33	(structure)	0.54	2.6	>50	1.2 67 257
34	(structure)	0.53	2.3	>50	1.3 62 274
35	(structure)	0.10	1.4	>50	1.3 62 274
(rac)-**36**	(structure)	1.8	20	>50	0.7 75 255
(rac)-**37**	(structure)	1.1	23	>50	0.9 75 255
38	(structure)	0.50	3.4	>50	1.4 75 295
39	(structure)	0.28	4.4	>50	1.9 75 295
40	(structure)	0.02	0.67	>50	2.4 62 294
41	(structure)	0.30	2.6	>50	2.7 62 322
42	(structure)	0.34	5.7	>50	2.7 62 322
43	(structure)	0.23	2.3	>50	2.3 62 322

[a]Generic structure shown in Scheme 2.

ophilicity efficiencies as exemplified by **35** (LE = 0.5; LLE = 5.7).

With a clear positional preference of the heteroatom, we evaluated six-membered heterocyclic linkers with heteroatoms located in meta and para positions (Table 4). The 5-pyrimidine **36** and 4-pyridazine **37**, each without substituents, were both relatively weak HDAC4 inhibitors, whereas addition of a 2-cyclopropyl substituent to the pyrimidine cap (**38**) improved biochemical and cell potency. Modeling suggested that introduction of this cyclopropane substituent in the meta-position relative to the biaryl junction may be preferred. The pyridazine **39** and in particular the cyclopropylpyridine **40** both demonstrated a significant improvement in potency (for **40**: HDAC4, 20 nM; cell (Lys-TFA), 670 nM). However, this compound showed poor metabolic stability in MLM (Cl$_{int}$ = 367 mL min^{-1} kg^{-1}) and was a potential substrate for P-gp (EER = 9.2; Table 5). Replacing the cyclopropyl by a CF$_3$ group (**41**) led to a pronounced drop in HDAC4 potency as illustrated by the CF$_3$-substituted pyridines **42** and **43**. Although this subseries of heterocyclic linkers exhibited good HDAC4 potency, most of the compounds displayed poor MLM intrinsic clearance and high P-gp efflux.

Evidence from our X-ray structures suggested that occupancy of the predominantly hydrophobic channel of the HDAC4 protein could be optimized by inclusion of a bicyclic linker group. Guided by docking studies, a number of bicyclic

Table 5. In Vitro ADME Data for Selected Heteroaromatic Linker Compounds Shown in Table 4

	R	cat. HDAC4 (μM)	cell-based activity (μM)		microsomal stability Cl_{int} (mL/min/kg)		MDCK-MDR1 (ratio; nm/s)		AlogP TPSA (Å²) M_w
			Lys-TFA	Lys-Ac	MLM	HLM	EER	$P_{app\ A\to B}$	
35		0.10	1.4	>50	>1297	<36	2.5	283	1.3 62 274
40		0.02	0.67	>50	367	<36	9.2	254	2.4 62 294
41		0.30	2.6	>50	-	-	4.7	200	2.7 62 322

Table 6. Structure, Activity, and in Vitro ADME Data for Fused Heteroaromatic Linkers[a]

	R	cat. HDAC4 (μM)	cell-based activity (μM)		microsomal stability Cl_{int} (mL/min/kg)		MDCK-MDR1 (ratio; nm/s)		AlogP TPSA (Å²) M_w
			Lys-TFA	Lys-Ac	MLM	HLM	EER	$P_{app\ A\to B}$	
44		1.5	7.1	>50	-	-	-	-	1.5 67 293
45		0.67	5.6	>50	-	-	-	-	1.7 67 293
46		0.20	1.7	>50	<65	<36	10	134	2.4 67 367
47		0.01	0.15	>50	>1297	54	5.4	451	2.9 62 324
48		0.04	0.41	>50	118	<36	18	362	3.1 76 334
49		0.02	0.16	>50	1259	<36	5.9	336	2.0 75 305
50		0.08	0.63	>50	<65	<36	7.4	307	3.3 75 373
51		0.02	0.13	>50	>1297	<36	5.1	334	3.0 75 345
52		0.03	0.11	>50	78	<36	12	267	3.0 75 345

[a]Generic structure shown in Scheme 2.

heteroaromatic groups were investigated (Table 6). Here, we found that a five-membered heterocyclic ring proximal to the cyclopropane core was deleterious for potency as illustrated by **44**, **45**, and **46**. The weak biochemical activity of imidazopyridine **44** confirmed our previous observation that heteroatoms placed close to the core were not tolerated. In contrast, fusion of heterocycles to the phenylene linker led to potent inhibitors as exemplified by the activity of benzothiazole **47** and quinoxaline **49**. Most of these compounds were relatively stable in human liver microsomes but not in mouse liver microsomes. While introduction of a CF_3 or a cyclopropyl substituent (in **50** and **52**) improved metabolic stability and retained biological activity, most of the compounds in this series were potential P-gp substrates.

In order to investigate the impact of a fused heterocycloalkyl ring system on potency and other properties, a number of analogues were synthesized and profiled as shown in Table 7. For benzodioxanes **53** and **54**, addition of a chlorine atom on the fused phenyl moiety increased potency, as expected from modeling studies, but introduced efflux by P-gp. Compounds **53** and **54** were unstable in mouse liver microsomes, with metabolism likely to occur at the ethylene bridge. The geminal dimethyl-substituted benzodioxane **55** was designed to block this potential metabolic soft spot and indeed demonstrated improved stability in MLM without a marked reduction in HDAC4 inhibitory activity. Modifying the ring heteroatom of the potent tetrahydroquinoline **56** resulted in a compound with high passive permeability in MDCK cells that was not a substrate of P-gp in vitro (EER = 1.7), despite the addition of a further hydrogen bond donor.

HDAC Selectivity. In order to understand the selectivity of these cyclopropane-based HDAC inhibitors, we investigated the inhibitory activity of selected compounds representing the different subchemotypes against a panel of other HDAC isoforms. Specifically, we compared HDAC4 activity with the other class IIa isoforms and class I HDACs 1, 2, 3, and 8, along

Table 7. Structure, activity, and in Vitro ADME Data for Partially Saturated Bicyclic Linkers[a]

	R	cat. HDAC4 (µM)	cell-based activity (µM)		microsomal stability Cl$_{int}$ (mL/min/kg)		MDCK-MDR1 (ratio; nm/s)		AlogP TPSA (Å²) M$_w$
			Lys-TFA	Lys-Ac	MLM	HLM	EER	P$_{app\ A\rightarrow B}$	
53		0.03	0.62	>50	>1297	197	1.1	437	2.3 68 311
54		0.02	0.13	>50	>1297	391	4.8	361	3.0 68 346
55		0.04	0.56	>50	236	97	5.1	170	3.5 68 374
56		0.04	0.47	>50	>1297	120	1.7	303	3.5 61 343
57		0.03	0.28	>50	<65	40	4.1	130	2.7 70 390

[a]Generic structure shown in Scheme 2.

Table 8. Selectivity Data for Representative Lead Molecules

	cat. HDAC4 (µM)	cat. HDAC5 (µM)	cat. HDAC7 (µM)	cat. HDAC9 (µM)	HDAC1 (µM)	HDAC2 (µM)	HDAC3 (µM)	HDAC6 (µM)	HDAC8 (µM)
(rac)-15	0.34	0.34	1.1	1.8			33	9.7	4.3
25	0.05	0.03	0.11	0.19	21		9.4	1.9	1.4
(rac)-26	0.09	0.05	0.22	0.37			26	5.3	5.3
31	0.02	0.004	0.03	0.04	32	43	12		0.36
33	0.54	0.15	0.46	0.79	>50	>50	25		6.7
40	0.02	0.03	0.12	0.26			18	5.6	4.8
49	0.02	0.007	0.01	0.03	22	>50	8.9		0.87
54	0.02	0.009	0.02	0.05	17	31	4.7		0.83
57	0.03	0.009	0.06	0.08	24	>50	16		1.5
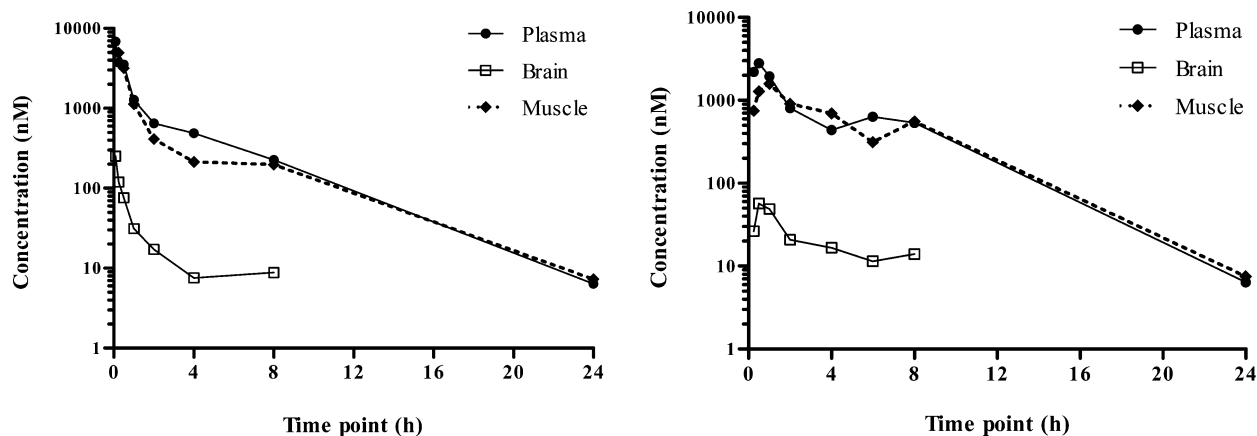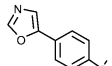
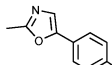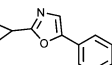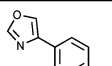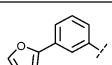**Figure 5.** Concentrations of **57** in plasma, brain, and muscle over time following a single iv administration at 5 mg/kg (left) and po administration at 10 mg/kg (right) to fed male C57Bl/6 mice.

with HDAC6 as a representative of class IIb (Table 8). As anticipated by the high homology within the catalytic site of the class IIa subfamily, only minor differences in activity were observed in most cases. Perhaps the most notable discrepancy was detected for the truncated pyridine **40**, whereby the compound was roughly 15-fold more active for HDAC4 compared to HDAC9. We have demonstrated that these cyclopropane molecules can differentiate class IIa HDACs from class I and class IIb subtypes, which confirmed our design principles of exploiting the lower pocket. Compounds demonstrated excellent biochemical HDAC4 versus class I

HDAC selectivities, in particular over HDACs 1, 2, and 3, with selectivity, albeit less pronounced, over HDAC8, a class I HDAC that resembles a class IIa enzyme in substrate recognition. For example, compound **31** displayed 2000-fold selectivity over HDAC2 (class I) and less than 20-fold selectivity versus HDAC8, whereas compound **40** showed 200-fold selectivity against the latter. Compounds demonstrated selectivity over HDAC6 (class IIb) in excess of 100-fold.

Pharmacokinetic in Vivo Studies. The benzopyrrolidinone **57** displayed good biochemical and cell-based potency and adequate metabolic stability in MLM and HLM. Its

Table 9. Phenyl Linker Scaffold with Oxazole Capping Groups: Regiochemistry and Substitution[a]

	R	cat. HDAC4 (μM)	cell-based activity (μM)		microsomal stability Cl_{int} (mL/min/kg)		MDCK-MDR1 (ratio; nm/s)		AlogP TPSA (Å^2) M_w
			Lys-TFA	Lys-Ac	MLM	HLM	EER	$P_{app\ A \to B}$	
31		0.02	0.22	>50	89	<36	2.4	442	2.2 76 320
58		0.03	0.33	>50	531	<36	3.4	460	2.5 76 334
59		0.04	0.30	>50	71	<36	4.0	255	3.2 76 360
60		0.06	0.50	>50	>1297	<36	3.6	466	2.4 76 320
61		0.04	0.39	>50	>1286	<36	6.0	484	2.2 76 320

[a]Generic structure shown in Schemes 1 and 2.

Table 10. Pharmacokinetic Parameters of 57, 31, and 59 after Administration to Fed Male C57Bl/6 mice

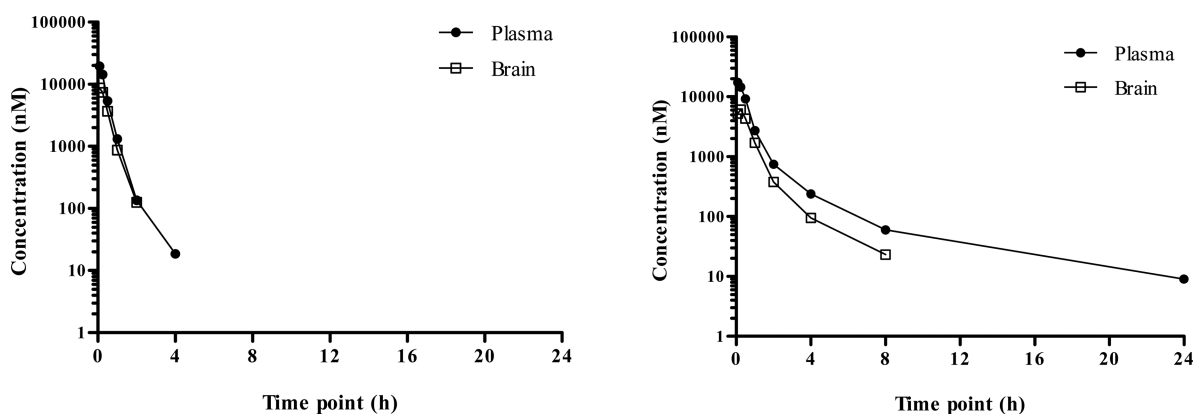| compd	compartment	po (10 mg/kg)					iv (5 mg/kg)		
		F (%)	AUCN (nM h kg/mg)	C_{max} (nM kg/mg)	T_{max} (h)	tissue/plasma	Cl_p (L h^{-1} kg^{-1})	Vd_{ss} (L/kg)	$T_{1/2}$ (h)
57	plasma	62	1100	280	0.5		1.4	4.6	3.2
	brain		17	5.7	0.5	0.01−0.04			
	muscle		1000	160	1	0.5−1.5			
31	plasma	84	1300	1200	0.5		2.0	0.74	0.4
	brain		700	670	0.5	0.2−1			
	muscle		810	730	0.5	0.2−1.3			
59	plasma	73	1500	810	0.5		1.4	1.6	1.7
	brain		390	200	1.0	0.3−0.6			
	muscle		1000	420	1	0.4−1.6			

Figure 6. Concentrations of **31** (left) and **59** (right) in plasma and brain over time following iv administration (6.3 and 7.1 mg/kg, respectively) to fed male C57Bl/6 mice.

moderate-to-high effective efflux ratio of 4 and relatively low passive permeability ($P_{appA \to B}$ = 130 nm/s) indicated that CNS exposure may be limited. With the aim of assessing the relationship between in vitro and in vivo pharmacokinetic data, the compound was evaluated in vivo in mice.

Following iv administration (5 mg/kg) of **57** to mice, moderate plasma clearance was observed (1.4 L h^{-1} kg^{-1}) with a moderate-to-large volume of distribution at steady state (4.6 L/kg) and a half-life of 3.2 h (Table 10). Following po

administration (10 mg/kg), absorption was rapid with the time of maximal concentration (T_{max}) occurring between 0.5 and 1 h for plasma, brain, and muscle (Figure 5). The compound displayed acceptable oral bioavailability (62%).

Brain concentrations were low relative to the plasma exposure (brain-to-plasma ratios of 0.01−0.04), and it was not possible to distinguish between compound in parenchyma versus contamination from residual blood in the brain homogenate. The low brain to plasma ratios observed for
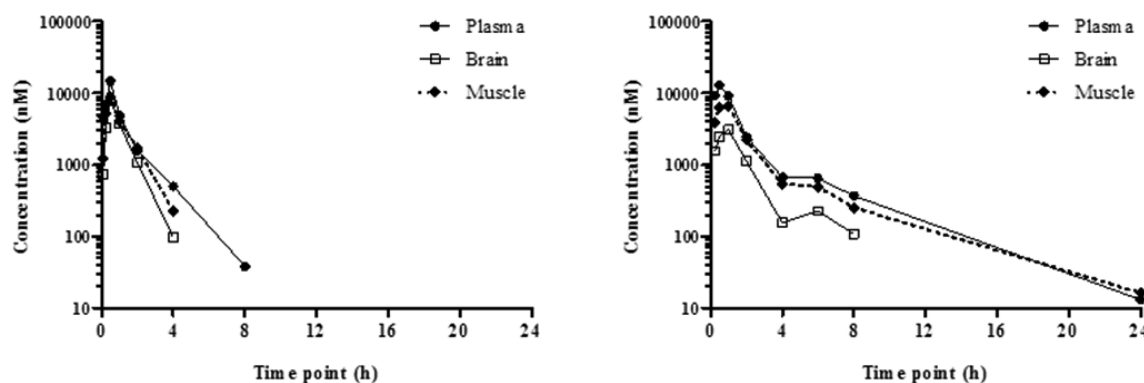
Figure 7. Concentrations of **31** (left) and **59** (right) in plasma, brain, and muscle over time following po administration (12 and 16 mg/kg, respectively) to fed male C57Bl/6 mice.

compound **57** are likely the consequence of both lower permeability and efflux by P-gp, suggesting that in our in vitro systems, an effective efflux ratio of ~4 combined with relatively low permeability ($P_{appA \rightarrow B}$ 130 nm/s) will translate to poor CNS exposure relative to plasma. Compound **57** was distributed to muscle tissue with muscle-to-plasma ratios ranging from 0.5 to 1.5 (AUCN = 1000 nM·h·kg/mg following oral administration) and thus may serve as a suitable tool molecule to interrogate peripheral HDAC4 (or class IIa isoforms) inhibition.

Optimization for potency, selectivity, metabolic stability, and minimal efflux by P-gp in a single molecule was challenging. The oxazole **31** fulfilled this criterion, but it was an inhibitor of human hepatic CYP450. Several close analogues were evaluated to address CYP450 inhibition. C(2) methylation of the oxazolyl element maintained HDAC4 potency (**58**) but resulted in much higher intrinsic clearance in MLM than **31** (Table 9). Blocking the oxazole 2-position diminished its potential for human CYP450 inhibition in vitro (IC_{50} values for **58**: CYP2C9, >100 μM; CYP2C19, >100 μM; CYP2D6, >39 μM). Other alkyl analogues were also found to be unstable in MLM. The cyclopropyl analogue **59**, however, retained good potency, was not a potent CYP inhibitor (IC_{50} values: CYP2C9, 23 μM; CYP2C19, >100 μM; CYP2D6, >45 μM), and was relatively stable in mouse liver microsomes (Cl_{int} = 71 mL min^{-1} kg^{-1}). However, its passive permeability was among the lowest for these analogues ($P_{appA \rightarrow B}$ = 255 nm/s), and the EER value was 4, higher than that of the unsubstituted oxazole **31** and similar to that of compound **57** which translated to poor brain exposure in mice.

The pharmacokinetic behavior of the unsubstituted oxazole **31** and its cyclopropyl analogue **59** was investigated. Following iv administration to mice (Table 10, Figure 6), both compounds displayed moderate plasma clearance and a low to moderate volume of distribution at steady state. Compound **59** exhibited an apparent biphasic elimination with a terminal half-life of 1.7 h measured between 2 and 8 h postdose. The pharmacokinetic profile of **31** appeared to have a single elimination phase with a half-life value of 0.4 h measured between 0.25 and 6 h postdose. However, the presence of a longer terminal phase for **31** at concentrations below the analytical limit of quantification cannot be discounted. The compounds were rapidly absorbed following an oral dose (Figure 7), with T_{max} in plasma at 0.5 h and oral bioavailability values of 84% and 73%. Metabolites related to epimerization at the core cyclopropane ring of **31** were not detected in circulation in the plasma.

Both compounds were distributed from plasma into brain tissue, with compound **31** displaying slightly higher distribution than **59** (brain to plasma ratios of 0.2−1.0 vs 0.3−0.6, respectively). This is consistent with the in vitro data that showed compound **59** had lower cell permeability and greater potential for efflux by P-gp than **31**. Both compounds had similar distribution to muscle tissue with muscle-to-plasma ratios ranging from 0.2 to 1.3 for compound **31** and from 0.4 to 1.6 for **59** (AUCN of 810 and 1000 nM·h·kg/mg following oral administration, respectively).

Total concentrations in brain tissue, determined from tissue homogenates, do not directly relate to target engagement. The unbound fraction of these two compounds in the presence of brain homogenate, as determined in vitro by equilibrium dialysis, was 0.026 for **31** and 0.0037 for **59**. Hence, when dosed at 10 mg/kg po, we estimated free concentrations of **31** to reach its cell-based IC_{50} value, whereas **59** requires administration at higher dosage to achieve free concentrations at or above its IC_{50}. However, estimation of free concentrations based on in vitro equilibrium dialysis data can be difficult to interpret and may not be a valid approach to determine the brain concentration necessary for target engagement. HDAC4 is an intracellular protein shuttling between nucleus and cytosol; therefore, steady-state drug concentrations in the HDAC4 environment may not be identical to that of the estimated extracellular levels in brain. Understanding the on and off rates of bound inhibitors is also important for estimating target coverage and more important than a free fraction determined in equilibrium against a buffer. Finally, in the absence of a pharmacodynamics marker, it is difficult to take into account whether concentrations corresponding to an in vitro determined IC_{20}, IC_{50}, or IC_{90} value will be required to exert a biological effect. These questions are currently being addressed and will be reported in due course.

■ CONCLUSIONS

Class IIa HDACs are large proteins with multiple functions including transcription factor binding, *N*-acetyllysine recognition, and perhaps weak deacetylation activity. Thus, a critical issue is whether or not occupancy of the class IIa HDAC catalytic domain with small molecules will be capable of replicating, either fully or in part, the beneficial effects of the class IIa HDAC genetic suppression studies proven to be efficacious in the various preclinical paradigms and so would provide a rationale for small molecule therapy. Given our interest in the development of HDAC4 inhibitors as a potential

therapeutic strategy for Huntington's disease, we developed molecules with optimized selectivity for class IIa over class I and class IIb isotypes and good brain and muscle exposure following oral administration. This optimization process was guided by crystallography and structure-based design. The introduction of a well-designed single amino acid substitution that maintains the molecular environment within the catalytic site has enabled provision of important structural information, i.e., with compound **31**. The data sets for compounds **25** and **31** confirmed the existence of a lower selectivity pocket and formed the basis for detailed docking studies. Selectivity over class I and class IIb has clearly been achieved within this compound series, whereas pharmacologically relevant selectivity levels over the other class IIa isoforms have been difficult, as predicted by their high similarity. Nevertheless, these molecules exhibit a very different profile from those of SAHA and other previously studied HDAC inhibitors and in particular do not interact with the class I isoforms which are very actively involved in chromatin remodeling and transcriptional regulation. Optimization of the ADME properties for CNS permeability constituted a challenge; however, balancing the predicted physicochemical properties led to molecules with suitable microsomal stability, and limited P-gp mediated efflux. This culminated in the identification of tool molecules with distribution to brain and muscle, the oxazoles **31** and **59**, for the evaluation of compound efficacy and proof of concept studies in disease models where deregulation of class II HDAC biology has been implicated. In addition, we identified a molecule (**57**) that is well distributed to muscle but does not partition into brain, for indications in which CNS activity may, in fact, be undesirable. Further in vitro and in vivo proof-of-concept experiments with these and other class IIa inhibitors will be reported in due course.

■ EXPERIMENTAL SECTION

General Comments on Experimental Data. All chemicals purchased from commercial suppliers were used as received. Flash chromatography was carried out with prepacked SiO$_2$ SNAP cartridges (KP-SIL) from Biotage using a Biotage Isolera Four system using gradient elution. Analytical thin-layer chromatography (TLC) was performed on silica using PolygramSIL G/UV254 with fluorescent indicator (200 μm thickness) and visualized under UV light. NMR spectra were recorded on a Bruker AV 400 (^{1}H, 400.13 MHz) instrument spectrometer and referenced in CDCl$_3$ to tetramethylsilane (0.00 ppm) and in DMSO-d_6 referenced to DMSO-d_5 (2.50 ppm). The following abbreviations are used: br = broad signal, s = singlet, br s = broad singlet, d = doublet, dd = doublet of doublets, t = triplet, q = quartet, m = multiplet. Preparative HPLC was performed on a Waters Sunfire OBD C18 10 μm column (150 mm × 19 mm), Phenomenex Luna phenylhexyl 10 μm column (150 mm × 21.2 mm), or a Waters Xbridge phenyl 5 μm column (100 mm × 19 mm), eluting with mixtures of water–acetonitrile or water–methanol, optionally containing a modifier (0.1% v/v formic acid or 10 mM ammonium bicarbonate). Low-resolution mass spectra were recorded on a Waters ZQ single quadrupole LCMS instrument in ESCi+, ESCi− mode or on a Quattro Micro LC–MS–MS instrument in ESCi+, ESCi− mode. All final compounds were purified to >95% chemical purity as assayed by HPLC/MS (detailed analytical methods in Supporting Information). HRMS experiments were performed on a Waters Acquity UPLC system and Waters Xevo G2 TOF mass spectrometer. Compounds were named with the aid of the Cambridgesoft Chemistry Cartridge (version 9.0.0.182) software. All reactions involving air- or moisture-sensitive reagents were performed under a nitrogen atmosphere using dried solvents and glassware. Racemic mixtures of the cyclopropyl core are denoted using asterisks, e.g., (1R*,2R*,3R*). Chirally pure compounds are denoted without asterisks, e.g., (1R,2R,3R).

***trans-N*-Hydroxy-2,3-diphenylcyclopropanecarboxamide (15).** To a stirred solution of 2,3-diphenylcyclopropanecarboxylic acid[68] (62 mg, 0.26 mmol), BOP (128 mg, 0.29 mmol), and triethylamine (0.10 mL, 0.78 mmol) in pyridine (1 mL) was added hydroxylamine hydrochloride (20 mg, 0.29 mmol). The reaction mixture was stirred at room temperature for 2 h. The reaction mixture was diluted with water (10 mL) and extracted into EtOAc (3 × 20 mL). The combined organic layers were washed with water (2 × 20 mL), dried (MgSO$_4$), and concentrated. The crude material was purified by preparative HPLC and PEAX cartridge (DCM–MeOH, 1:1). The solvent was removed in vacuo to afford the title compound (25 mg, 38%) as a white solid. LCMS (ES$^+$) 254 (M + H)$^+$, (ES$^−$) 252 (M − H)$^−$, t_R = 2.97 min (analytical method 1). ^{1}H NMR δ (ppm) (DMSO-d_6): 10.55 (1 H, s), 8.69 (1 H, s), 7.36–7.16 (10 H, m), 3.09 (1 H, dd, J = 6.8, 5.4 Hz), 2.83 (1 H, dd, J = 9.6, 6.8 Hz), 2.20 (1 H, dd, J = 9.6, 5.4 Hz).

General Procedure A for the Synthesis of 16−61 (Hydroxamic Acid Formation). To a stirred solution of ester (0.30 mmol) in THF/MeOH (1:1, 3 mL) were added hydroxylamine (0.2 mL, 50% aqueous solution, 3.00 mmol) and potassium hydroxide (0.60 mmol). The mixture was stirred at room temperature for 2 h, neutralized with 1 M HCl$_{(aq)}$, and extracted with DCM. The combined organic layers were washed with brine (10 mL), passed through a phase separator, and concentrated.

(2R,3S)-N-Hydroxy-2,3-diphenylcyclopropanecarboxamide (16). The synthesis involved following procedure A from (2R,3S)-ethyl 2,3-diphenylcyclopropanecarboxylate[69](180 mg, 0.68 mmol). The residual gum obtained after workup was dissolved in DCM (10 mL) and the resulting white precipitate was collected by vacuum filtration and washed with DCM (2 × 5 mL) to give the title compound (55 mg, 32%). LCMS (ES$^+$) 254 (M + H)$^+$, (ES$^−$) 252 (M − H)$^−$, t_R = 3.00 min (analytical method 1). ^{1}H NMR δ (ppm) (DMSO-d_6): 10.76 (1 H, s), 8.94 (1 H, s), 7.17–7.04 (6 H, m), 7.02–6.94 (4 H, m), 2.83 (2 H, d, J = 5.4 Hz), 2.52 (1 H obscured by DMSO).

(1S,2R)-N-Hydroxy-2-phenylcyclopropanecarboxamide (17). The synthesis involved following procedure A from (1S,2R)-ethyl 2-phenylcyclopropanecarboxylate[70] (550 mg, 2.89 mmol). The residual gum obtained after workup was dissolved in DCM (10 mL), and the resulting white precipitate was collected by vacuum filtration and washed with DCM (2 × 5 mL). Purification by preparative HPLC gave the title compound (105 mg, 20%). LCMS (ES$^+$) 178 (M + H)$^+$, t_R = 2.66 min (analytical method 1). ^{1}H NMR δ (ppm) (DMSO-d_6): 10.43 (1 H, s), 8.55 (1 H, s), 7.21 (4 H, d, J = 4.3 Hz), 7.16–7.09 (1 H, m), 2.36 (1 H, dd, J = 16.6, 8.3 Hz), 1.87–1.80 (1 H, m), 1.54–1.48 (1 H, m), 1.24–1.16 (1 H, m). HRMS (ESI) calcd for C$_{21}$H$_{24}$N$_2$O$_2$ [M + H]$^+$ 178.0868, found 178.0871.

(1S,2S)-N-Hydroxy-2-phenylcyclopropanecarboxamide (18). The synthesis involved following procedure A from (1S,2S)-ethyl 2-phenylcyclopropanecarboxylate[70] (17) (1.05 g, 5.53 mmol). The residual gum obtained after workup was dissolved in DCM (10 mL), and the resulting white precipitate was collected by vacuum filtration and washed with DCM (2 × 5 mL) to give the title compound (723 mg, 74%). LCMS (ES$^+$) 178 (M + H)$^+$, t_R = 2.22 min (analytical method 2). ^{1}H NMR δ (ppm) (DMSO-d_6): 10.60 (1 H, s), 8.81 (1 H, s), 7.34–7.25 (2 H, m), 7.24–7.11 (3 H, m), 2.29–2.22 (1 H, m), 1.73–1.66 (1 H, m), 1.41–1.33 (1 H, m), 1.28–1.21 (1 H, m).

General Procedure B for the Synthesis of 6a, 6c, and 13a−l. To a stirred solution of triethyl phosphonoacetate (24.4 mmol) in THF (30 mL) at 0 °C was added sodium hydride (24.4 mmol) portionwise. The mixture was stirred for 1 h before addition of aldehyde (12.2 mmol). The reaction mixture was allowed to warm to room temperature, stirred for 17 h, quenched with water (50 mL), and extracted into EtOAc (2 × 50 mL). The organic layers were combined and washed with water (2 × 50 mL), dried (MgSO$_4$), filtered, and concentrated.

General Procedure C for the Synthesis of 7a−c, 14a−k, and 14a′−q′ (Cyclopropanation Reaction). A mixture of sulfonium salt (8.92 mmol), enoate (5.96 mmol), and 12-crown-4 (8.92 mmol) in DCM (20 mL) was cooled to −20 °C. LiHMDS (8.92 mL) was then

added dropwise. After complete addition, the mixture was warmed to room temperature, stirred for 2 h, and quenched with water (30 mL). The biphasic mixture was separated, and the organic layers were washed with brine (2 × 30 mL), separated, dried (MgSO$_4$), filtered, and concentrated.

General Procedure D for the Synthesis of 9a−c (Buchwald Reaction). To a stirred solution of aryl bromide (0.76 mmol) and amine (0.86 mmol) in dioxane (4 mL) were added xantphos (0.048 mmol), cesium carbonate (1.66 mmol), and Pd$_2$(dba)$_3$ (0.024 mmol). The mixture was stirred for 16 h at 90 °C, diluted with water, and extracted into DCM (20 mL). The organic layers were passed through a phase separator and concentrated, and the crude mixture was purified by flash silica column chromatography.

General Procedure E for the Synthesis of 9d and 9f−g (Suzuki Coupling). To a stirred solution of 7a or 7b (3.02 mmol) in dioxane (5 mL) was added bis-pinacolatodiboron (3.32 mmol), Pd(dppf)Cl$_2$ (0.30 mmol), and potassium acetate (15.1 mmol). The mixture was degassed with nitrogen and then heated to 100 °C for 2 h. The reaction mixture was diluted with water (20 mL) and extracted into DCM (2 × 20 mL). The organic layers were passed through a phase separator and concentrated. The crude residue was dissolved in dioxane, and an aliquot (0.66 mmol) was added to a reaction tube. To this were added heterocyclic halide (0.69 mmol), Pd(PPh$_3$)$_4$ (0.066 mmol), and aqueous Na$_2$CO$_3$ (5 mL, 1 M solution). The mixture was heated at 100 °C for 2 h. The mixture was diluted with water (10 mL) and extracted into DCM (20 mL). The organic layers were passed through a phase separator and concentrated.

General Procedure F for the Synthesis of 9i, 9j, and 9l (Stille Coupling). A mixture of aryl bromide (0.67 mmol), stannane (0.81 mmol), and Pd(PPh$_3$)$_4$ (0.034 mmol) in 1,4-dioxane (4 mL) was heated in the microwave at 150 °C for 1 h. The mixture was concentrated and purified by flash silica column chromatography.

General Procedure G for the Synthesis of 9m and 9n (Oxazole Coupling). A stirred solution of 7b or 7a (1.46 mmol), oxazole (2.42 mmol), Pd(Oac)$_2$ (0.07 mmol), di-*tert*-butyl(2′,4′,6′-triisopropyl-3,4,5,6-tetramethylbiphenyl-2-yl)phosphine (0.146 mmol), K$_2$CO$_3$ (4.38 mmol), and pivalic acid (0.58 mmol) in DMA (7.5 mL) was degassed with nitrogen for 15 min before heating at 110 °C for 16 h. The mixture was cooled and diluted with DCM (20 mL) and washed with water (3 × 30 mL). The organic layers were passed through a phase separator and concentrated.

General Procedure H for the Synthesis of 13a′, 13b′, 13d′−k′, 13m′, 13n′, 13p′, 13q′ (Heck Reaction). A stirred mixture of aryl bromide (10.0 mmol), ethyl acrylate (15.0 mmol), palladium acetate (1.00 mmol), P(*o*-tol)$_3$ (2.00 mmol), and triethylamine (20.0 mmol) in MeCN (50 mL) was degassed with nitrogen for 15 min and heated to 80 °C for 3−18 h. The reaction mixture was cooled and the MeCN removed in vacuo. The residue was partitioned between DCM and water and the organic layers were passed through a phase separator and concentrated.

(1R*,2R*,3R*)-2-(4-(3,3-Dimethylazetidin-1-yl)phenyl)-N-hydroxy-3-phenylcyclopropanecarboxamide (19). The synthesis involved following procedure D from 7b (250 mg, 0.76 mmol) and 3,3-dimethylazetidine (105 mg, 0.86 mmol). Purification by flash silica column chromatography (gradient elution *i*-hex/EtOAc 0−100%) gave (1R*,2R*,3R*)-methyl-2-(4-(3,3-dimethylazetidin-1-yl)phenyl)-3-phenylcyclopropanecarboxylate (9a) as a clear oil (210 mg, 59%) which was progressed into the next step. The synthesis involved following procedure A from 9a (200 mg, 0.59 mmol). Purification by preparative HPLC gave the title compound as a white solid (23 mg, 14%). LCMS (ES$^+$) 337 (M + H)$^+$, t_R = 3.42 min (analytical method 1). ^{1}H NMR δ (ppm) (DMSO-d_6): 10.49 (1 H, s), 8.63 (1 H, s), 7.33−7.20 (4 H, m), 7.19−7.12 (1 H, m), 7.05 (2 H, d, J = 8.2 Hz), 6.37 (2 H, d, J = 8.2 Hz), 3.48 (4 H, s), 2.97 (1 H, dd, J = 6.9, 5.4 Hz), 2.68 (1 H, dd, J = 9.5, 6.9 Hz), 2.06 (1 H, dd, J = 9.5, 5.4 Hz), 1.27 (6 H, s). HRMS (ESI) calcd for C$_{21}$H$_{24}$N$_2$O$_2$ [M + H]$^+$ 337.1916, found 337.1899.

(1R*,2R*,3R*)-2-(4-(2-Oxa-6-azaspiro[3.3]heptan-6-yl)-phenyl)-N-hydroxy-3-phenylcyclopropanecarboxamide (20). The synthesis involved following procedure D from 7b (250 mg,

0.76 mmol) and 2-oxa-6-azaspiro[3.3]heptane formate salt (160 mg, 0.86 mmol). Purification by flash silica column chromatography (gradient elution *i*-hex/EtOAc 0−100%) gave (1R*,2R*,3R*)-methyl-2-(4-(2-oxa-6-azaspiro[3.3] heptan-6-yl)phenyl)-3-phenylcyclopropanecarboxylate (9b) as a clear oil [210 mg, 59%, LCMS (ES$^+$) 364 (M + H)$^+$], which was progressed into the next step. The synthesis involved following procedure A from 9b (214 mg, 0.61 mmol). Purification by preparative HPLC gave the title compound as a white solid (23 mg, 14%). LCMS (ES$^+$) 351 (M + H)$^+$, t_R = 8.07 min (analytical method 3). ^{1}H NMR δ (ppm) (DMSO-d_6): 10.50 (1 H, s), 8.64 (1 H, d, J = 1.8 Hz), 7.31 (2 H, d, J = 7.6 Hz), 7.28−7.21 (2 H, m), 7.19−7.08 (3 H, m), 6.60 (2 H, d, J = 8.2 Hz), 3.70−3.61 (4 H, m), 3.48−3.39 (4 H, m), 2.99 (1 H, dd, J = 6.9, 5.4 Hz), 2.70 (1 H, dd, J = 9.5, 6.9 Hz), 2.08 (1 H, dd, J = 9.5, 5.4 Hz). HRMS (ESI) calcd for C$_{21}$H$_{22}$N$_2$O$_3$ [M + H]$^+$ 351.1708, found 351.1706.

(1R*,2R*,3R*)-N-Hydroxy-2-(4-(3,3-difluoropyrrolidin-1-yl)-phenyl)-3-phenylcyclopropanecarboxamide (21). The synthesis involved following procedure D from 7b (250 mg, 0.76 mmol) and 3,3-difluoropyrrolidine (124 mg, 0.86 mmol). Purification by flash silica column chromatography (gradient elution *i*-hex/EtOAc 0−100%) gave (1R*,2R*,3R*)-methyl-2-(4-(3,3-difluoropyrrolidin-1-yl)-phenyl)-3-phenylcyclopropanecarboxylate (9c) as a clear oil (210 mg, 59%) which was progressed into the next step. The synthesis involved following procedure A from 9c (205 mg, 0.57 mmol). Purification by preparative HPLC gave the title compound as a white solid (35 mg, 17%). LCMS (ES$^+$) 359 (M + H)$^+$, t_R = 9.27 min (analytical method 5). ^{1}H NMR δ (ppm) (DMSO-d_6): 10.50 (1 H, s), 8.64 (1 H, d, J = 1.8 Hz), 7.31 (2 H, d, J = 7.6 Hz), 7.25 (2 H, t, J = 7.4 Hz), 7.19−7.08 (3 H, m), 6.60 (2 H, d, J = 8.2 Hz), 3.66 (2 H, t, J = 13.4 Hz), 3.44 (2 H, m), 2.99 (1 H, m), 2.70−2.65 (2 H, m), 2.33 (1 H, m), 2.08 (1 H, dd, J = 9.5, 5.4 Hz). HRMS (ESI) calcd for C$_{20}$H$_{20}$F$_2$N$_2$O$_2$ [M + H]$^+$ 359.1571, found 359.1565.

(1R*,2R*,3R*)-N-Hydroxy-2-phenyl-3-(4-(pyridazin-3-yl)-phenyl)cyclopropanecarboxamide (22). The synthesis involved following procedure A from 9d (68 mg, 0.21 mmol). Purification using an Isolute anion exchange SPE (elution DCM−MeOH, 1:1) gave the title compound as a white solid (49 mg, 70%). LCMS (ES$^+$) 332 (M + H)$^+$, t_R = 2.95 min (analytical method 1). ^{1}H NMR δ (ppm) (DMSO-d_6): 10.59 (1 H, s), 9.20 (1 H, dd, J = 4.8, 1.5 Hz), 8.71 (1 H, s), 8.23 (1 H, dd, J = 8.6, 1.5 Hz), 8.14 (2 H, d, J = 8.1 Hz), 7.78 (1 H, dd, J = 8.6, 4.9 Hz), 7.48 (2 H, d, J = 8.1 Hz), 7.37 (2 H, d, J = 7.5 Hz), 7.32−7.24 (2 H, m), 7.22−7.16 (1 H, m), 3.19 (1 H, dd, J = 6.8, 5.4 Hz), 2.93 (1 H, dd, J = 9.6, 6.8 Hz), 2.31 (1 H, dd, J = 9.6, 5.4 Hz). HRMS (ESI) calcd for C$_{20}$H$_{17}$N$_3$O$_2$ [M + H]$^+$ 332.1399, found 332.1393.

(1R*,2R*,3R*)-N-Hydroxy-2-phenyl-3-(4-(pyrimidin-5-yl)-phenyl)cyclopropanecarboxamide (23). To a stirred solution of 7b (130 mg, 0.39 mmol) in MeOH/DME (1:5, 5 mL) were added Pd(PPh$_3$)$_4$ (45 mg, 0.039 mmol), cesium fluoride (119 mg, 0.78 mmol), and 5-pyrimidineboronic acid (58 mg, 0.47 mmol). The mixture was degassed with nitrogen for 15 min before heating in the microwave at 120 °C for 1 h. The reaction mixture was diluted with H$_2$O (10 mL) and extracted into DCM (50 mL). The organic layers were dried over MgSO$_4$, filtered, and concentrated. Purification by column chromatography (gradient elution *i*-hex to 5% EtOAc in *i*-hex) gave (1R*,2R*,3R*)-methyl-2-phenyl-3-(4-(pyrimidin-5-yl)phenyl)-cyclopropane carboxylate (9e) as a colorless oil [120 mg, 93%, LCMS (ES$^+$) 345 (M + H)$^+$] which was progressed to the next step. The synthesis involved following procedure A from 9e (120 mg, 0.36 mmol). Purification by flash silica column chromatography (gradient elution DCM to 5% MeOH in DCM) and Isolute anion exchange SPE (elution DCM−MeOH, 1:1) gave the title compound as a white solid (21 mg, 17%). LCMS (ES$^+$) 332 (M + H)$^+$, t_R = 3.07 min (analytical method 1). ^{1}H NMR δ (ppm) (DMSO-d_6): 10.60 (1 H, s), 9.18 (1 H, s), 9.15 (2 H, s), 8.72 (1 H, s), 7.79 (2 H, d, J = 8.1 Hz), 7.45 (2 H, d, J = 8.1 Hz), 7.35 (2 H, d, J = 7.6 Hz), 7.27 (2 H, t, J = 7.6 Hz), 7.19 (1 H, t, J = 7.2 Hz), 3.18 (1 H, dd, J = 6.8, 5.4 Hz), 2.92 (1 H, dd, J = 9.6, 6.8 Hz), 2.27 (1 H, dd, J = 9.6, 5.4 Hz). HRMS (ESI) calcd for C$_{20}$H$_{17}$N$_3$O$_2$ [M + H]$^+$ 332.1399, found 332.1392.

(1R*,2R*,3R*)-N-Hydroxy-2-phenyl-3-(4-(pyrimidin-2-yl)-phenyl)cyclopropanecarboxamide (24). The synthesis involved

following procedure E from the crude boronate derived from **7b** (274 mg), and 2-chloropyrimidine (87 mg, 0.76 mmol). Purification by flash silica column chromatography (gradient elution *i*-hex to 25% EtOAc in *i*-hex) gave (1*R**,2*R**,3*R**)-methyl 2-phenyl-3-(4-(pyrimidin-2-yl)-phenyl)cyclopropanecarboxylate (**9f**) as a pale yellow oil [110 mg, 46%, LCMS (ES⁺) 345 (M + H)⁺] which was progressed to the next step. The synthesis involved following procedure A from **9f** (110 mg, 0.33 mmol). Purification by column chromatography (gradient elution DCM to 5% MeOH in DCM) gave the title compound as a white solid (75 mg, 67%). LCMS (ES+) 332 (M + H)⁺, (ES⁻) 330 (M + H)⁻, t_R = 2.78 min (analytical method 1). ¹H NMR δ (ppm) (DMSO-d_6): 10.59 (1 H, s), 8.90 (2 H, d, *J* = 4.8 Hz), 8.72 (1 H, s), 8.36 (2 H, d, *J* = 8.2 Hz), 7.48−7.40 (3 H, m), 7.36 (2 H, d, *J* = 7.6 Hz), 7.27 (2 H, t, *J* = 7.6 Hz), 7.19 (1 H, t, *J* = 7.3 Hz), 3.18 (1 H, dd, *J* = 6.8, 5.4 Hz), 2.93 (1 H, dd, *J* = 9.6, 6.8 Hz), 2.30 (1 H, dd, *J* = 9.6, 5.4 Hz). HRMS (ESI) calcd for $C_{20}H_{17}N_3O_2$ [M + H]⁺ 332.1399, found 332.1390.

(1*R**,2*R**,3*R**)-2-(4-(5-Fluoropyrimidin-2-yl)phenyl)-*N*-hydroxy-3-phenylcyclopropanecarboxamide (25). The synthesis involved following procedure E from the crude boronate derived from **7b** (250 mg) and 2-chloro-5-fluoropyrimidine (91 mg, 0.69 mmol). Purification by flash silica column chromatography (gradient elution *i*-hex to 10% EtOAc in *i*-hex) gave (1*R**,2*R**,3*R**)-methyl 2-(4-(5-fluoropyrimidin-2-yl)phenyl)-3-phenylcyclopropanecarboxylate (**9g**) as a colorless oil [240 mg, 100%, LCMS (ES⁺) 363 (M + H)⁺], which was progressed to the next step. The synthesis involved following procedure A from **9g** (220 mg, 0.63 mmol). Purification by flash silica column chromatography (gradient elution DCM to 5% MeOH in DCM) gave the title compound as a white solid (81 mg, 37%). LCMS (ES⁺) 350 (M + H)⁺, t_R = 3.13 min (analytical method 1). ¹H NMR δ (ppm) (DMSO-d_6): 10.58 (1 H, s), 8.97 (2 H, d, *J* = 0.8 Hz), 8.70 (1 H, s), 8.30 (2 H, d, *J* = 8.2 Hz), 7.44 (2 H, d, *J* = 8.2 Hz), 7.36 (2 H, d, *J* = 7.6 Hz), 7.27 (2 H, t, *J* = 7.5 Hz), 7.20 (1 H, d, *J* = 7.2 Hz), 3.18 (1 H, dd, *J* = 6.7, 5.6 Hz), 2.93 (1 H, dd, *J* = 9.6, 6.7 Hz), 2.30 (1 H, dd, *J* = 9.6, 5.4 Hz). HRMS (ESI) calcd for $C_{20}H_{16}FN_3O_2$ [M + H]⁺ 350.1304, found 350.1298.

(1*R**,2*R**,3*R**)-2-(3-(5-Fluoropyrimidin-2-yl)phenyl)-*N*-hydroxy-3-phenylcyclopropanecarboxamide (26). The synthesis involved following procedure E from the crude boronate derived from **7a** (300 mg) and 2-chloro-5-fluoropyrimidine (107 mg, 0.81 mmol). Purification by flash silica column chromatography (gradient elution *i*-hex to 10% EtOAc in *i*-hex) gave (1*R**,2*R**,3*R**)-ethyl 2-(3-(5-fluoropyrimidin-2-yl)phenyl)-3-phenylcyclopropanecarboxylate (**9h**) as a colorless oil [140 mg, 50%, LCMS (ES⁺) 363 (M + H)⁺], which was progressed to the next step. The synthesis involved following procedure A from **9h** (140 mg, 0.39 mmol). Purification by flash silica column chromatography (gradient elution DCM to 7% MeOH in DCM) and preparative HPLC gave the title compound as a racemic mixture (12 mg, 9%). LCMS (ES⁺) 350 (M + H)⁺, t_R = 3.61 min (analytical method 1). ¹H NMR δ (ppm) (DMSO-d_6): 10.59 (1 H, s), 9.01 (2 H, s), 8.71 (1 H, s), 8.20 (2 H, t, *J* = 4.0 Hz), 7.51−7.48 (2 H, m), 7.37 (2 H, d, *J* = 7.6 Hz), 7.29−7.24 (2 H, m), 7.20 (1 H, d, *J* = 7.3 Hz), 3.22 (1 H, dd, *J* = 6.8, 5.5 Hz), 2.85 (1 H, dd, *J* = 9.6, 6.8 Hz), 2.32 (1 H, dd, *J* = 9.6, 5.4 Hz). HRMS (ESI) calcd for $C_{20}H_{16}FN_3O_2$ [M + H]⁺ 350.1304, found 350.1307.

(1*R**,2*R**,3*R**)-*N*-Hydroxy-2-(4-(1-methyl-1*H*-imidazol-2-yl)-phenyl)-3-phenylcyclopropanecarboxamide (27). The synthesis involved following procedure F from **7b** (222 mg, 0.67 mmol) and 1-methyl-2-(tributylstannyl)imidazole (300 mg, 0.81 mmol). Purification by flash silica column chromatography (gradient elution DCM to 10% MeOH in DCM) gave (1*R**,2*R**,3*R**)-methyl-2-(4-(1-methyl-1*H*-imidazol-2-yl)phenyl)-3-phenylcyclopropanecarboxamide (**9i**) as a yellow solid [187 mg, 84%, LCMS (ES⁺) 347 (M + H)⁺] which was progressed to the next step. The synthesis involved following procedure A from **9i** (187 mg, 0.56 mmol). Crystallization from DCM and trituration with MeOH gave the title compound as a white solid (98 mg, 53%). LCMS (ES⁺) 334 (M + H)⁺, t_R = 9.74 min (analytical method 3). ¹H NMR δ (ppm) (DMSO-d_6): 10.58 (1 H, s), 8.70 (1 H, s), 7.65 (2 H, d, *J* = 8.1 Hz), 7.44−7.31 (4 H, m), 7.30−7.24 (3 H, m), 7.23−7.15 (1 H, m), 6.99 (1 H, d, *J* = 1.1 Hz), 3.75 (3

H, s), 3.19−3.13 (1 H, dd, *J* = 6.8, 5.4 Hz), 2.90 (1 H, dd, *J* = 9.6, 6.8 Hz), 2.26 (1 H, dd, *J* = 9.6, 5.4 Hz). HRMS (ESI) calcd for $C_{20}H_{19}N_3O_2$ [M + H]⁺ 334.1555, found 334.1543.

(1*R**,2*R**,3*R**)-*N*-Hydroxy-2-(4-(5-methyl-1*H*-imidazol-2-yl)-phenyl)-3-phenylcyclopropanecarboxamide (28). The synthesis involved following procedure F from crude boronate derived from **7b** (1.5 mmol) and 2-bromo-4-methylimidazole (242 mg, 1.5 mmol). Purification by flash silica column chromatography (gradient elution DCM−MeOH 0−10%) gave (1*R**,2*R**,3*R**)-methyl 2-(4-(5-methyl-1*H*-imidazol-2-yl)phenyl)-3-phenylcyclopropanecarboxylate (**9j**) as a yellow oil (285 mg). The crude material was used in the next step [LCMS (ES⁺) 335 (M + H)⁺]. The synthesis involved following procedure A from **9j** (280 mg, 0.84 mmol). Purification by preparative HPLC gave the title compound as a white solid (4.8 mg, 1% yield over three steps). LCMS (ES⁺) 334 (M + H)⁺, t_R = 7.93 min (analytical method 3). ¹H NMR δ (ppm) (DMSO-d_6): 10.62 (1 H, s), 8.42 (1 H, s), 7.88 (2 H, d, *J* = 8.0 Hz), 7.41−7.28 (6 H, m), 7.25−7.20 (1 H, m), 6.84 (1 H, s), 3.16 (1 H, dd, *J* = 6.9, 5.5 Hz), 2.92 (1 H, dd, *J* = 9.4, 6.7 Hz), 2.31−2.20 (4 H, m), OH not observed. HRMS (ESI) calcd for $C_{20}H_{19}N_3O_2$ [M + H]⁺ 334.1555, found 334.1545.

(1*R*,2*R*,3*R*)-2-(3-Fluoro-4-(5-methyl-1*H*-imidazol-2-yl)-phenyl)-*N*-hydroxy-3-phenylcyclopropanecarboxamide (29). To the crude boronate derived from **7c** (1.5 mmol) in DME/MeOH (4:1, 10 mL) were added 2-bromo-4-methyl-1*H*-imidazole (353 mg, 2.20 mmol), cesium fluoride (333 mg, 2.20 mmol), and Pd(PPh₃)₄ (84 mg, 0.073 mmol). This mixture was heated under microwave irradiation at 110 °C for 1 h. The reaction mixture was cooled, diluted with water, and extracted with DCM. The organic layers were combined, washed with water, dried (MgSO₄), filtered, and concentrated to give a brown gum. Purification by flash silica column chromatography (gradient elution *i*-hex to 100% EtOAc in *i*-hex) gave (1*R**,2*R**,3*R**)-ethyl 2-(3-fluoro-4-(5-methyl-1*H*-imidazol-2-yl)-phenyl)-3-phenylcyclopropanecarboxylate (**9k**) as an off white solid [134 mg, 25%, 7:3 trans/cis, LCMS (ES⁺) 365 (M + H)⁺], which was progressed to the next step. The synthesis involved following procedure A from **9k** (154 mg, 0.42 mmol) to yield an off white gum (200 mg). Purification by preparative HPLC gave the racemic product as a pale yellow solid (16 mg, 10%). Preparative chiral purification gave the title compound as a formate salt (3 mg, 2%, Chiralpak IC 40/60 IPA/MeOH (50/50/0.1% formic acid)/heptane 5.0 mL/min). LCMS (ES⁺) 352 (M + H)⁺, 2.29 min (analytical method 1). ¹H NMR δ (ppm) (DMSO-d_6): 11.88 (0.5 H, s), 11.80 (0.5 H, s), 10.56 (1 H, s), 8.70 (1 H, s), 8.52 (1 H, s), 7.90 (1 H, q, *J* = 8.6 Hz), 7.34 (2 H, d, *J* = 7.6 Hz), 7.29−7.24 (3 H, m), 7.19 (2 H, s), 6.93 (0.5 H, s), 6.74 (0.5 H, s), 3.15 (1 H, dd, *J* = 6.8, 5.2 Hz), 2.93 (1 H, dd, *J* = 9.7, 6.8 Hz), 2.26 (1 H, dd, *J* = 9.7, 5.2 Hz), 2.24 (1.5 H, s), 2.17 (1.5 H, s). HRMS (ESI) calcd for $C_{20}H_{18}FN_3O_2$ [M + H]⁺ 352.1461, found 352.1464.

(1*R**,2*R**,3*R**)-*N*-Hydroxy-2-(4-(oxazol-2-yl)phenyl)-3-phenylcyclopropanecarboxamide (30). The synthesis involved following procedure F from **7b** (250 mg, 0.75 mmol) and 2-(tri-*n*-butylstannyl)oxazole (0.230 mL, 1.1 mmol). Purification by flash silica column chromatography (gradient elution DCM to 10% MeOH in DCM) afforded (1*R**,2*R**,3*R**)-methyl-2-(4-(oxazol-2-yl)phenyl)-3-phenylcyclopropanecarboxamide (**9l**) as a white solid [175 mg, 73%, LCMS (ES⁺) 334 (M + H)⁺] which was progressed to the next step. The synthesis involved following procedure A from **9l** (160 mg, 0.50 mmol). Crystallization from MeOH gave the title compound as a white solid (71 mg, 45%). LCMS (ES⁺) 321 (M + H)⁺, t_R = 2.80 min (analytical method 1). ¹H NMR δ (ppm) (DMSO-d_6): 10.58 (1 H, s), 8.70 (1 H, s), 8.21 (1 H, d, *J* = 0.8 Hz), 7.94 (2 H, d, *J* = 8.1 Hz), 7.45 (2 H, d, *J* = 8.1 Hz), 7.39−7.33 (3 H, m), 7.31−7.23 (2 H, m), 7.22−7.15 (1 H, m), 3.20−3.13 (1 H, m), 2.91 (1 H, dd, *J* = 9.6, 6.8 Hz), 2.28 (1 H, dd, *J* = 9.6, 5.3 Hz). HRMS (ESI) calcd for $C_{19}H_{16}N_2O_3$ [M + H]⁺ 321.1239, found 321.1229.

(1*R*,2*R*,3*R*)-*N*-Hydroxy-2-(4-(oxazol-5-yl)phenyl)-3-phenyl-cyclopropanecarboxamide (31). The synthesis involved following procedure A from **9m**. Purification by flash silica column chromatography (gradient elution DCM to 5% MeOH in DCM) gave the racemic mixture as a white solid (88 mg, 29%). Preparative

chiral HPLC gave the title compound (Chiralpak IC 20/80 EtOH (0.1 formic acid)/heptane, 1.0 mL/min, t_R = 18.7 min). LCMS (ES$^+$) 321 (M + H)$^+$, t_R = 2.77 min (analytical method 1). ^{1}H NMR δ (ppm) (DMSO-d_6): 10.63 (1 H, s), 8.76 (1 H, s), 8.49 (1 H, s), 7.76–7.72 (3 H, m), 7.47–7.36 (4 H, m), 7.35–7.29 (2 H, m), 7.25–7.20 (1 H, m), 3.18 (1 H, dd, J = 6.8, 5.4 Hz), 2.94 (1 H, dd, J = 9.6, 6.8 Hz), 2.30 (1 H, dd, J = 9.6, 5.4 Hz). HRMS (ESI) calcd for $C_{19}H_{16}N_2O_3$ [M + H]$^+$ 321.1239, found 321.1235.

(1S*,2R*,3R*)-2-Cyclopentyl-N-hydroxy-3-phenyl-cyclopropanecarboxamide (32). The synthesis involved following procedure A from **14a** (1.05 g, 4.06 mmol). Purification by flash silica column chromatography (gradient elution DCM to 4% MeOH in DCM) and preparative HPLC gave the title compound as a white solid (23 mg, 9%). LCMS (ES$^+$) 246 (M + H)$^+$, t_R = 3.18 min (analytical method 1). ^{1}H NMR δ (ppm)(DMSO-d_6): 10.57 (1 H, s), 8.76 (1 H, s), 7.35–7.27 (2 H, m), 7.24–7.18 (3 H, m), 1.88 (1 H, t, J = 5.0 Hz), 1.71–1.60 (1 H, m), 1.58–1.47 (2 H, m), 1.50–1.16 (8 H, m). HRMS (ESI) calcd for $C_{15}H_{19}NO_2$ [M + H]$^+$ 246.1494, found 246.1491.

(1R,2R,3R)-N-Hydroxy-2-(1-methyl-1H-pyrazol-4-yl)-3-phenylcyclopropanecarboxamide (33). The synthesis involved following procedure A from **14b** (493 mg, 1.83 mmol). Purification by flash silica column chromatography (gradient elution DCM to 5% MeOH in DCM) and then preparative HPLC gave the racemic mixture as a white solid (235 mg, 50%). Preparative chiral HPLC gave the title compound (Chiralpak IC 30/70 IPA/MeOH (50/50/0.1% formic acid)/heptane, 1.0 mL/min, t_R = 10.3 min). LCMS (ES$^+$) 258 (M + H)$^+$, (ES$^-$) 256 (M + H)$^-$, t_R = 2.65 min (analytical method 1). ^{1}H NMR δ (ppm) (DMSO-d_6): 10.50 (1 H, s), 8.63 (1 H, s), 7.61 (1 H, s), 7.34 (1 H, s), 7.28–7.13 (5 H, m), 3.78 (3 H, s), 2.86 (1 H, dd, J = 6.9, 5.3 Hz), 2.63 (1 H, dd, J = 9.4, 6.9 Hz), 1.97 (1 H, dd, J = 9.4, 5.3 Hz). HRMS (ESI) calcd for $C_{14}H_{15}N_3O_2$ [M + H]$^+$ 258.1242, found 258.1237.

(1R,2R,3S)-N-Hydroxy-2-(5-methylthiazol-2-yl)-3-phenyl-cyclopropanecarboxamide (34). The synthesis involved following procedure A from **14c** (92 mg). Purification by flash silica column chromatography (gradient elution DCM to 4% MeOH in DCM) and preparative HPLC gave the racemic compound (38 mg, 86% based on purity of SM). Preparative chiral purification gave the title compound (Chiralpak IA 15/85 MeOH (50/50/0.1 formic acid)/heptane 1.0 mL/min, t_R = 12.3 min). LCMS (ES$^+$) 275 (M + H)$^+$, t_R = 3.07 min (analytical method 1). ^{1}H NMR δ (ppm) (DMSO-d_6): 10.55 (1 H, s), 8.63 (1 H, s), 7.29 (1 H, d, J = 1.4 Hz), 7.26–7.22 (3 H, m), 7.21–7.16 (2 H, m), 7.15–7.09 (1 H, m), 3.31 (1 H, dd, J = 6.34, 5.2 Hz), 2.87 (1 H, dd, J = 9.7, 6.4 Hz), 2.40 (1 H, dd, J = 9.7, 5.2 Hz), 2.34 (3 H, d, J = 1.2 Hz). HRMS (ESI) calcd for $C_{14}H_{14}N_2O_2S$ [M + H]$^+$ 275.0854, found 275.0853.

(1R,2R,3S)-N-Hydroxy-2-(5-methylthiazol-2-yl)-3-phenyl-cyclopropanecarboxamide (35). The synthesis involved following procedure A from **14i** (92 mg). Purification by flash silica column chromatography (gradient elution DCM to 4% MeOH in DCM) and preparative HPLC gave the racemic compound (38 mg, 86% based on purity of SM). Preparative chiral purification gave the title compound (Chiralpak IA 15/85 MeOH (50/50/0.1 formic acid)/heptane 1.0 mL/min, t_R = 12.3 min). LCMS (ES$^+$) 275 (M + H)$^+$, t_R = 3.07 min (analytical method 1). ^{1}H NMR δ (ppm) (DMSO-d_6): 10.55 (1 H, s), 8.63 (1 H, s), 7.29 (1 H, d, J = 1.4 Hz), 7.26–7.22 (3 H, m), 7.21–7.16 (2 H, m), 7.15–7.09 (1 H, m), 3.31 (1 H, dd, J = 6.34, 5.2 Hz), 2.87 (1 H, dd, J = 9.7, 6.4 Hz), 2.40 (1 H, dd, J = 9.7, 5.2 Hz), 2.34 (3 H, d, J = 1.2 Hz). HRMS (ESI) calcd for $C_{14}H_{14}N_2O_2S$ [M + H]$^+$ 275.0854, found 275.0850.

(1R*,2R*,3R*)-N-Hydroxy-2-phenyl-3-(pyrimidin-5-yl)-cyclopropanecarboxamide (36). The synthesis involved following procedure A from **14d** (270 mg, 1.08 mmol). Purification by flash silica chromatography (gradient elution DCM to 7% MeOH in DCM) and reversed phase HPLC gave the title compound as a yellow solid (9 mg, 5%). LCMS (ES$^+$) 256 (M + H)$^+$, t_R = 2.52 min (analytical method 1). ^{1}H NMR δ (ppm) (DMSO-d_6): 10.61 (1 H, s), 9.06 (1 H, s), 8.79 (2 H, s), 8.72 (1 H, s), 7.34 (2 H, d, J = 7.6 Hz), 7.27 (2 H, t, J = 7.5 Hz), 7.22–7.17 (1 H, m), 3.15 (1 H, dd, J = 6.8, 5.5 Hz), 3.04 (1

H, dd, J = 9.6, 6.9 Hz), 2.37 (1 H, dd, J = 9.7, 5.5 Hz). HRMS (ESI) calcd for $C_{14}H_{13}N_3O_2$ [M + H]$^+$ 256.1086, found 256.1083.

(1R*,2R*,3R*)-N-Hydroxy-2-phenyl-3-(pyridazin-4-yl)-cyclopropanecarboxamide (37). The synthesis involved following procedure A from **14a′** (45 mg, 0.17 mmol). Purification by flash silica column chromatography (gradient elution DCM to 4% MeOH in DCM) and reversed phase HPLC gave the title compound as a white solid (3 mg, 21%). LCMS (ES$^+$) 256 (M + H)$^+$, t_R = 7.02 min (analytical method 3). ^{1}H NMR δ (ppm) (DMSO-d_6): 10.69 (1 H, s), 9.34 (1 H, s), 9.15 (1 H, d, J = 5.4 Hz), 8.81 (1 H, s), 7.63–7.61 (1 H, m), 7.40–7.30 (4 H, m), 7.27–7.24 (1 H, m), 3.22 (1 H, dd, J = 5.2, 6.4 Hz), 3.13 (1 H, dd, J = 6.4, 9.5 Hz), 2.45 (1 H, dd, J = 9.5, 5.3 Hz). HRMS (ESI) calcd for $C_{14}H_{13}N_3O_2$ [M + H]$^+$ 256.1086, found 256.1081.

(1R,2R,3R)-2-(2-Cyclopropylpyrimidin-5-yl)-N-hydroxy-3-phenylcyclopropanecarboxamide (38). The synthesis involved following procedure A from **14b′** (310 mg). Purification by preparative HPLC gave the racemic compound (30 mg, 10%). Preparative chiral purification gave the title compound (Chiralpak IC 40/60 IPA/MetOH (0.1% formic acid)/heptane 1.0 mL/min). LCMS (ES$^+$) 296 (M + H)$^+$, t_R = 2.93 min (analytical method 1). ^{1}H NMR δ (ppm) (DMSO-d_6): 10.48 (1 H, s), 8.59 (1 H, s), 8.51–8.48 (6 H, m), 7.25 (3 H, d, J = 7.6 Hz), 7.21–7.16 (3 H, m), 7.12 (1 H, d, J = 7.23 Hz), 2.99 (1 H, dd, J = 6.7, 5.4 Hz), 2.86 (1 H, dd, J = 9.5, 6.8 Hz), 2.21 (1 H, dd, J = 9.6, 5.5 Hz), 2.12–2.08 (1 H, m), 0.96–0.91 (2 H, m), 0.91–0.87 (2 H, m). HRMS (ESI) calcd for $C_{17}H_{17}N_3O_2$ [M + H]$^+$ 296.1399, found 296.1399.

(1R,2R,3R)-2-(6-Cyclopropylpyridazin-4-yl)-N-hydroxy-3-phenylcyclopropanecarboxamide (39). The synthesis involved following procedure A from **14o′** (0.1 g, 0.3 mmol). Preparative chiral purification gave the title compound (Chiralpak IC 30/70 [IPA/MeOH (50/50/0.1% formic acid)]/heptane 5.0 mL/min, t_R = 28.95 min). LCMS (ES$^+$) 296 (M + H)$^+$, t_R = 2.82 min (analytical method 1). ^{1}H NMR δ (ppm) (DMSO-d_6): 10.63 (1 H, s), 9.07 (1 H, d, J = 2.1 Hz), 8.76 (1 H, s), 7.42–7.35 (3 H, m), 7.32 (2 H, t, J = 7.4 Hz), 7.25 (1 H, t, J = 7.1 Hz), 3.17–3.08 (2 H, m), 2.45 (1 H, dd, J = 9.5, 5.6 Hz), 2.28–2.21 (1 H, m), 1.15–1.11 (4 H, m). HRMS (ESI) calcd for $C_{17}H_{17}N_3O_2$ [M + H]$^+$ 296.1399, found 296.1406.

(1R,2R,3R)-2-(2-Cyclopropylpyridin-4-yl)-N-hydroxy-3-phenylcyclopropanecarboxamide (40). The synthesis involved following procedure A from **14f′** (330 mg, 1.07 mmol). Purification by flash silica column chromatography (gradient elution DCM to 5% MeOH in DCM) gave the racemic mixture as a white solid (60 mg, 19%). Preparative chiral HPLC gave the title compound (Chiralpak IC 30/70 IPA/MeOH (50/50/0.1 formic acid)/heptane, 1.0 mL/min, t_R = 9.6 min). LCMS (ES$^+$) 295 (M + H)$^+$, (ES$^-$) 293 (M − H)$^-$, t_R = 2.12 min (analytical method 1). ^{1}H NMR δ (ppm) (DMSO-d_6): 10.65 (1 H, s), 8.78 (1 H, s), 8.32 (1 H, d, J = 5.1 Hz), 7.37 (2 H, d, J = 7.6 Hz), 7.34–7.28 (2 H, m), 7.25 (2 H, d, J = 8.2 Hz), 7.07 (1 H, dd, J = 5.2, 1.7 Hz), 3.10 (1 H, dd, J = 6.7, 5.6 Hz), 2.99 (1 H, dd, J = 9.7, 6.7 Hz), 2.34 (1 H, dd, J = 9.7, 5.6 Hz), 2.12–2.07 (1 H, m), 0.98–0.93 (4 H, m). HRMS (ESI) calcd for $C_{18}H_{18}N_2O_2$ [M + H]$^+$ 295.1446, found 295.1450.

(1R,2R,3R)-N-Hydroxy-2-phenyl-3-(2-(trifluoromethyl)-pyridin-4-yl)cyclopropanecarboxamide (41). The synthesis involved following procedure A from **14h′** (130 mg, 0.41 mmol). Purification by flash silica column chromatography (gradient elution DCM to 5% MeOH in DCM) followed by preparative HPLC gave the racemic mixture as a white solid (90 mg, 68%). Preparative chiral HPLC gave the title compound (Chiralpak IC 20/80 IPA/MeOH (50/50/0.1 formic acid)/heptane, 1.0 mL/min, t_R = 10.3 min). LCMS (ES$^+$) 323 (M + H)$^+$, t_R = 3.50 min (analytical method 1). ^{1}H NMR δ (ppm) (DMSO-d_6): 10.66 (1 H, s), 8.81 (1 H, s), 8.71 (1 H, d, J = 5.0 Hz), 7.92 (1 H, s), 7.70 (1 H, d, J = 5.1 Hz), 7.40 (2 H, d, J = 7.5 Hz), 7.32 (2 H, t, J = 7.5 Hz), 7.27–7.22 (1 H, m), 3.35 (1H, dd, J = 6.6, 5.4 Hz), 3.16 (1 H, dd, J = 9.5, 6.6 Hz), 2.48 (1 H, dd, J = 9.5, 5.4 Hz). HRMS (ESI) calcd for $C_{16}H_{13}F_3N_2O_2$ [M + H]$^+$ 323.1007, found 323.1006.

(1R,2R,3R)-N-Hydroxy-2-phenyl-3-(6-(trifluoromethyl)-pyridin-3-yl)cyclopropanecarboxamide (42). The synthesis in-

volved following procedure A from compound **14j′** (720 mg, 2.24 mmol). Purification by flash silica column chromatography (gradient elution DCM to 5% MeOH in DCM) followed by preparative HPLC gave the racemic mixture as a white solid (83 mg, 11%). Preparative chiral HPLC gave the title compound (Chiralpak IC 20/80 IPA/MeOH (50/50/0.1 formic acid)/heptane, 1.0 mL/min, t_R = 14.5 min). LCMS (ES$^+$) 323 (M + H)$^+$, t_R = 8.60 min (analytical method 3). ^{1}H NMR δ (ppm) (DMSO-d_6): 10.70 (1 H, s), 8.84 (1 H, s), 8.82 (1H, s), 8.02−7.97 (1 H, m), 7.91 (1 H, d, J = 8.2 Hz), 7.40 (2 H, d, J = 7.6 Hz), 7.33 (2 H, t, J = 7.5 Hz), 7.28−7.22 (1 H, m), 3.32 (1 H, dd, J = 6.7 and 5.6 Hz), 3.09 (1 H, dd, J = 9.7, 6.8 Hz), 2.43 (1 H, dd, J =9.7 and 5.6 Hz). HRMS (ESI) calcd for $C_{16}H_{13}F_3N_2O_2$ [M + H]$^+$ 323.1007, found 323.1013.

(1R,2R,3R)-N-Hydroxy-2-phenyl-3-(5-(trifluoromethyl)-pyridin-3-yl)cyclopropanecarboxamide (43). The synthesis involved following procedure A from **14l′** (250 mg, 0.78 mmol). Purification by flash silica column chromatography (gradient elution DCM to 5% MeOH in DCM) followed by preparative HPLC gave the racemic mixture as a white solid (83 mg, 11%). Preparative chiral HPLC gave the title compound (Chiralpak IC 20/80 EtOH (0.1% formic acid)/heptane, 1.0 mL/min, t_R = 11.3 min). LCMS (ES$^+$) 323 (M + H)$^+$, t_R = 3.30 min (analytical method 1). ^{1}H NMR δ (ppm) (DMSO-d_6): 10.64 (1 H, s), 8.96 (1 H, s), 8.88 (1 H, s), 8.79 (1 H, s), 8.15 (1 H, s), 7.41 (2 H, d, J = 7.6 Hz), 7.32 (2 H, t, J = 7.4 Hz), 7.24 (1 H, t, J = 7.2 Hz), 3.41 (1 H, obscured by water), 3.15 (1 H, dd, J = 9.8, 6.9 Hz), 2.44 (1 H, dd, J = 9.8, 5.4 Hz). HRMS (ESI) calcd for $C_{16}H_{13}F_3N_2O_2$ [M + H]$^+$ 323.1007, found 323.1012.

(1R,2R,3R)-N-Hydroxy-2-(imidazo[1,2-a]pyridin-2-yl)-3-phenylcyclopropanecarboxamide (44). The synthesis involved following procedure A from **14a** (430 mg, 1.4 mmol) to yield a yellow gum. Purification by preparative HPLC gave the racemic product as a white solid (118 mg, 29%). Preparative chiral purification gave the title compound (Chiralpak IA 20/80 IPA/MeOH(50/50/0.1% formic acid)/heptane 5.0 mL/min). LCMS (ES$^+$) 294 (M + H)$^+$, 2.07 min (analytical method 1). ^{1}H NMR δ (ppm) (DMSO-d_6): 10.60 (1 H, s), 8.68 (1 H, s), 8.52 (1 H, d, J = 6.7 Hz), 7.99 (1 H, s), 7.50 (1 H, d, J = 9.1 Hz), 7.39 (2 H, d, J = 7.6 Hz), 7.33−7.18 (4 H, m), 6.89 (1 H, m,), 3.25 (1 H, dd, J = 6.5, 5.3 Hz), 2.96 (1 H, dd, J = 9.5, 6.5 Hz), 2.48 (1 H, dd, J = 9.6, 5.2 Hz). HRMS (ESI) calcd for $C_{17}H_{15}N_3O_2$ [M + H]$^+$ 294.1242, found 294.1245.

(1R,2R,3R)-N-Hydroxy-2-phenyl-3-(pyrazolo[1,5-a]pyridin-2-yl)cyclopropanecarboxamide (45). The synthesis involved following procedure A from **14f** (624 mg, 2.04 mmol) to yield a yellow gum (650 mg). Purification by preparative HPLC gave the racemic product as a pale yellow solid (378 mg, 63%). Preparative chiral purification gave the title compound (Chiralpak IC 50/50 IPA/MeOH (50/50/0.1% formic acid)/heptane 5.0 mL/min). LCMS (ES$^+$) 294 (M + H)$^+$, 3.37 min (analytical method 1). ^{1}H NMR δ (ppm) (DMSO-d_6): 10.64 (1 H, s), 8.78 (1 H, s), 8.10 (1 H, d, J = 2.4 Hz), 7.66 (1 H, d, J = 8.8 Hz), 7.46 (2 H, d, J = 7.5 Hz), 7.30 (2 H, t, J = 7.4 Hz), 7.21 (2 H, t, J = 7.6 Hz), 6.80 (1 H, d, J = 6.8 Hz), 6.71 (1 H, d, J = 2.3 Hz), 3.77 (1 H, dd, J = 6.9, 5.6 Hz), 3.05 (1 H, dd, J = 9.5, 6.9 Hz), 2.52−2.48 (1H, obscured by DMSO). HRMS (ESI) calcd for $C_{17}H_{15}N_3O_2$ [M + H]$^+$ 294.1242, found 294.1238.

(1R,2R,3R)-N-Hydroxy-2-phenyl-3-(6-(trifluoromethyl)-imidazo[2,1-b]thiazol-2-yl)cyclopropanecarboxamide (46). The synthesis involved following procedure A from **14c′** (158 mg, 0.42 mmol). Purification by preparative HPLC gave the racemic compound (55 mg, 36%). Preparative chiral purification gave the title compound (Chiralpak IC 30/70 [IPA/MeOH (50/50/0.1% formic acid)]/heptane 1.0 mL/min, t_R = 7.8 min). LCMS (ES$^+$) 368 (M + H)$^+$, t_R = 3.46 min (analytical method 1). ^{1}H NMR δ (ppm) (DMSO-d_6): 10.57 (1 H, s), 8.66 (1 H, s), 8.25 (1 H, s), 7.92 (1 H, s), 7.26−7.09 (5 H, m), 3.21 (1 H, dd, obscured by water peak), 2.85 (1 H, dd, J = 9.8, 6.7 Hz), 2.23 (1 H, dd, J = 9.8, 5.3 Hz). HRMS (ESI) calcd for $C_{16}H_{12}F_3N_3O_2S$ [M + H]$^+$ 368.0680, found 368.0687.

(1R,2R,3R)-N-hydroxy-2-(2-methylbenzo[d]thiazol-5-yl)-3-phenylcyclopropanecarboxamide (47). Following procedure A from **14d′** (680 mg, 2.02 mmol) gave a yellow glass (846 mg). Purification by preparative HPLC gave the racemic product as an off

white solid (450 mg, 69%). An amount of 200 mg sent to preparative chiral purification gave the title compound as an off-white solid (95 mg, 47%) (Chiralpak IC 40/60 IPA/MeOH (50/50/0.1% formic acid)/heptane 5.0 mL/min). LCMS (ES$^+$) 325 (M + H)$^+$, 3.37 min (analytical method 1). ^{1}H NMR δ (ppm) (DMSO-d_6): 10.56 (1 H, s), 8.69 (1 H, s), 7.96 (1 H, d, J = 1.8 Hz), 7.85 (1 H, d, J = 8.4 Hz), 7.41−7.33 (3 H, m), 7.31−7.23 (2 H, m), 7.19 (1 H, dd, J = 7.2, 7.2 Hz), 3.23 (1 H, dd, J = 6.8, 5.4 Hz), 2.92 (1 H, dd, J = 9.6, 6.8 Hz), 2.79 (3 H, s), 2.27 (1 H, dd, J = 9.6, 5.4 Hz). HRMS (ESI) calcd for $C_{18}H_{16}N_2O_2S$ [M + H]$^+$ 325.1010, found 325.1018.

(1R,2R,3R)-2-(2-cyclopropylbenzo[d]oxazol-6-yl)-N-hydroxy-3-phenylcyclopropanecarboxamide (48). The synthesis involved following procedure A from **14l** (240 mg, 0.69 mmol) to yield an orange glass (265 mg). Purification by preparative HPLC gave the racemic product as an off white solid (11 mg, 9%). Preparative chiral purification gave the title compound as a off white solid (Chiralpak IC 40/60 IPA/MeOH (50/50/0.1% formic acid)/heptane 5.0 mL/min). LCMS (ES$^+$) 335 (M + H)$^+$, 3.39 min (analytical method 1). ^{1}H NMR δ (ppm) (DMSO-d_6):10.55 (1 H, s), 8.68 (1 H, s), 7.56−7.52 (2 H, m), 7.36−7.31 (2 H, m), 7.30−7.22 (3 H, m), 7.21−7.15 (1 H, m), 3.22 (1 H, dd, J = 6.9, 5.36 Hz), 2.90 (1 H, dd, J = 9.5, 6.9 Hz), 2.29−2.21 (2 H, m), 1.20−1.09 (4 H, m).

(1R,2R,3R)-N-Hydroxy-2-phenyl-3-(quinoxalin-6-yl)-cyclopropanecarboxamide (49). The synthesis involved following procedure A from **14g** (490 mg, 1.54 mmol). Purification by preparative HPLC gave the racemic compound (110 mg, 36%). Preparative chiral purification gave the title compound [Chiralpak IC 40/60 IPA/MeOH (50/50/0.1% formic acid)/heptane 1.0 mL/min]. LCMS (ES$^+$) 306 (M + H)$^+$, t_R = 2.96 min (analytical method 1). ^{1}H NMR δ (ppm) (DMSO-d_6): 10.64 (1 H, s), 8.99 (1 H, d, J = 1.8 Hz), 8.95 (1 H, d, J = 1.8 Hz), 8.75 (1 H, s), 8.12 (1 H, d, J = 8.6 Hz), 8.03 (1 H, s), 7.87 (1 H, dd, J = 8.7, 2.0 Hz), 7.45 (2 H, d, J = 7.5 Hz), 7.33 (2 H, t, J = 7.5 Hz), 7.27−7.22 (1 H, m), 3.43 (1 H, dd, J = 6.8, 5.4 Hz), 3.10 (1 H, dd, J = 9.7, 6.8 Hz), 2.49 (1 H, dd, J = 9.7, 5.4 Hz). HRMS (ESI) calcd for $C_{18}H_{15}N_3O_2$ [M + H]$^+$ 306.1242, found 306.1241.

(1R,2R,3R)-N-Hydroxy-2-phenyl-3-(3-(trifluoromethyl)-quinoxalin-6-yl)cyclopropanecarboxamide (50). The synthesis involved following procedure A from **14p′** (178 mg, 2.16 mmol). The target compound was obtained after preparative HPLC purification followed by chiral HPLC purification (13.7 mg) (Chiralpak IC 20/80 [IPA/MeOH (50/50/0.1% formic acid)]/heptane 1.0 mL/min, t_R = 9.2 min). LCMS (ES$^+$) 374 (M + H)$^+$, t_R = 3.68 min (analytical method 1). ^{1}H NMR δ (ppm) (DMSO-d_6): 10.53 (1 H, s), 9.30 (1 H, s), 8.64 (1 H, s), 8.16 (1 H, d, J = 8.7 Hz), 8.09 (1 H, s), 7.98 (1 H, d, J = 8.8 Hz), 7.33 (2 H, d, J = 7.58 Hz), 7.21 (2 H, t, J = 7.50 Hz), 7.15−7.12 (1 H, m), 3.37 (1 H, dd, J = 6.7, 5.4 Hz), 3.06 (1 H, dd, J = 9.7, 6.7 Hz), 2.44−2.41 (1 H, dd, obscured by DMSO). HRMS (ESI) calcd for $C_{19}H_{14}F_3N_3O_2$ [M + H]$^+$ 374.1116, found 374.1119.

(1R,2R,3R)-2-(3-cyclopropylquinoxalin-6-yl)-3-phenyl-cyclopropanecarbohydroxamic Acid (51). The synthesis involved following procedure A from **14m′** (384g, 1.07 mmol). Purification by flash silica column chromatography (gradient elution DCM to 10% MeOH in DCM) and preparative HPLC gave the racemic compound (172 mg, 46%). Preparative chiral purification gave the title compound as an off white solid (Chiralpak IC 30/70 EtOH (0.1% formic acid)/ heptane 5.0 mL/min, t_R = 9.67 min). LCMS (ES$^+$) 346 (M + H)$^+$, t_R = 3.47 min (analytical method 1). ^{1}H NMR δ (ppm) (DMSO-d_6): 10.60 (1 H, s), 8.97−8.84 (1 H, m), 8.72 (1 H, s), 7.95−7.85 (2 H, m), 7.72 (1 H, dd, J = 8.7, 2.1 Hz), 7.39 (2 H, d, J = 7.6 Hz), 7.28 (2 H, dd, J = 7.6, 7.3 Hz), 7.20 (1 H, dd, J = 7.3, 7.3 Hz), 3.35 (1 H, dd, partly obscured by water peak), 3.03 (1 H, dd, J = 9.6, 6.8 Hz), 2.44−2.35 (2 H, m), 1.20−1.12 (4 H, m). HRMS (ESI) calcd for $C_{21}H_{19}N_3O_2$ [M + H]$^+$ 346.1556, found 346.1558.

(1R,2R,3R)-2-(2-Cyclopropylquinoxalin-6-yl)-3-phenyl-cyclopropanecarbohydroxamic Acid (52). The synthesis involved following procedure A from **14n′** (129 mg, 0.37 mmol). Purification by flash silica column chromatography (gradient elution DCM to 10% MeOH in DCM) and preparative HPLC gave the racemic compound (129 mg, 48%). Preparative chiral purification gave the title compound

as an off white solid (Chiralpak IC 40/60 EtOH (50/50/0.1% formic acid)/heptane 1.0 mL/min, t_R = 9.38 min). LCMS (ES$^+$) 346 (M + H)$^+$, t_R = 3.52 min (analytical method 1). ^{1}H NMR δ (ppm) (DMSO-d_6): 10.58 (1 H, s), 8.88 (1 H, s), 8.72 (1 H, s), 7.99 (1 H, d, J = 8.6 Hz), 7.77 (1 H, s), 7.69 (1 H, dd, J = 8.6, 2.1 Hz), 7.39 (2 H, d, J = 7.6 Hz), 7.28 (2 H, dd, J = 7.6, 7.3 Hz), 7.20 (1 H, d, J = 7.3 Hz), 3.02 (1 H, dd, J = 9.7, 6.9 Hz), 1.21–1.13 (4 H, m). Peaks were not seen in the region 2.65–2.35 (3H, m, obscured by DMSO). HRMS (ESI) calcd for $C_{21}H_{19}N_3O_2$ [M + H]$^+$ 346.1556, found 346.1559.

(1R,2R,3R)-2-(2,3-Dihydrobenzo[b][1,4]dioxin-6-yl)-N-hydroxy-3-phenylcyclopropanecarboxamide (53). The synthesis involved following procedure A from compound **14k** (652 mg, 2.01 mmol). Purification by flash silica column chromatography (gradient elution DCM to 5% MeOH in DCM) gave the racemic mixture as a white solid (420 mg, 67%). Preparative chiral HPLC gave the title compound (Chiralpak IC 30/70 IPA/MeOH (50/50/0.1% formic acid)/heptane, 1.0 mL/min, t_R = 8.1 min). LCMS (ES$^+$) 312 (M + H)$^+$, t_R = 8.59 min (analytical method 4). ^{1}H NMR δ (ppm) (DMSO-d_6): 10.57 (1 H, s), 8.73 (1 H, s), 7.35 (2 H, d, J = 7.59 Hz), 7.29 (2 H, t, J = 7.5 Hz), 7.24–7.17 (1 H, m), 6.85 (1 H, d, J = 8.5 Hz), 6.80–6.74 (2 H, m), 4.26 (4 H, s), 3.02 (1 H, dd, J = 6.8, 5.4 Hz), 2.78 (1 H, dd, J = 9.6, 6.8 Hz), 2.14 (1 H, dd, J = 9.6, 5.4 Hz). HRMS (ESI) calcd for $C_{18}H_{17}NO_4$ [M + H]$^+$ 312.1236, found 312.1243.

(1R,2R,3R)-2-(8-Chloro-2,3-dihydrobenzo[b][1,4]dioxin-6-yl)-N-hydroxy-3-phenylcyclopropanecarboxamide (54). The synthesis involved following procedure A from **14h** (484 mg, 1.35 mmol). Purification by flash silica column chromatography (gradient elution DCM to 5% MeOH in DCM) and then preparative HPLC gave the racemic product as a white solid (174 mg, 37%). Preparative chiral HPLC gave the title compound (Chiralpak IC 20/80 IPA/MeOH (50/50/0.1% formic acid)/heptane, 1.0 mL/min, t_R = 10.4 min). LCMS (ES$^+$) 346, 348 (M + H)$^+$, t_R = 3.57 min (analytical method 1). ^{1}H NMR δ (ppm) (DMSO-d_6): 10.50 (1 H, s), 8.68 (1 H, s), 7.31 (2 H, d, J = 7.6 Hz), 7.25 (2 H, t, J = 7.4 Hz), 7.21–7.13 (1 H, m), 6.93 (1 H, d, J = 2.1 Hz), 6.77 (1 H, d, J = 2.1 Hz), 4.34–4.26 (4 H, m), 3.00 (1 H, dd, J = 6.8, 5.4 Hz), 2.79 (1 H, dd, J = 9.6, 6.8 Hz), 2.14 (1 H, dd, J = 9.8, 5.4 Hz). HRMS (ESI) calcd for $C_{18}H_{16}ClNO_4$ [M + H]$^+$ 346.0846, found 346.0853.

(1R,2R,3R)-2-(8-Chloro-3,3-dimethyl-2,3-dihydrobenzo[b]-[1,4]dioxin-6-yl)-N-hydroxy-3-phenylcyclopropane-carboxamide (55). The synthesis involved following procedure A from **14j** (0.2 g, 0.54 mmol). Preparative chiral purification gave the title compound (Chiralpak IC 30/70 [IPA/MeOH (50/50/0.1% formic acid)]/heptane 5.0 mL/min, t_R = 15.6 min). LCMS (ES$^+$) 374 (M + H)$^+$, t_R = 7.50 min (analytical method 1). ^{1}H NMR δ (ppm) (DMSO-d_6): 10.48 (1 H, s), 8.67 (1 H, s), 7.30 (2 H, d, J = 7.4 Hz), 7.24 (2 H, t, J = 7.4 Hz), 7.17 (1 H, d, J = 7.4 Hz), 6.91 (1 H, d, J = 2.1 Hz), 6.73 (1 H, d, J = 2.1 Hz), 4.02 (2 H, s), 2.99 (1 H, dd, J = 6.8, 5.0 Hz), 2.79 (2 H, dd, J = 9.4, 6.8 Hz), 2.13 (1 H, dd, J = 9.4, 5.3 Hz), 1.29 (6 H, s). HRMS (ESI) calcd for $C_{20}H_{20}ClNO_4$ [M + H]$^+$ 374.1159, found 374.1151.

(1R,2R,3R)-2-(8-Chloro-1,2,3,4-tetrahydroquinolin-6-yl)-N-hydroxy-3-phenylcyclopropanecarboxamide (56). Following procedure A from **14e′** (136 mg, 0.38 mmol) yielded a yellow glass (200 mg). Purification by preparative HPLC gave the racemic product as an off white glass (44 mg, 33%). Preparative chiral purification gave the title compound (Chiralpak IC 20/80 IPA/MeOH (50/50/0.1% formic acid)/heptane 5.0 mL/min). LCMS (ES$^+$) 343 (M + H)$^+$. ^{1}H NMR δ (ppm) (DMSO-d_6): 10.46 (1 H, s), 8.64 (1 H, s), 7.32–7.19 (4 H, m), 7.19–7.12 (1 H, m), 6.94 (1 H, s), 6.76 (1 H, s), 5.42 (1 H, s), 3.25 (2 H, s), 2.91 (1 H, dd, J = 6.8, 5.4 Hz), 2.72–2.64 (3 H, m), 2.05 (1 H, dd, J = 9.6, 5.4 Hz), 1.81–1.75 (2 H, m). HRMS (ESI) calcd for $C_{19}H_{19}ClN_2O_2$ [M + H]$^+$ 343.1213, found 343.1224.

(1R,2R,3R)-N-Hydroxy-2-(1-oxo-2-(2,2,2-trifluoroethyl)-isoindolin-5-yl)-3-phenylcyclopropanecarboxamide (57). The synthesis involved following procedure A from **14g′** (gradient elution DCM to 6% MeOH in DCM), and then preparative HPLC gave the racemic mixture as a white solid. Preparative chiral HPLC gave the title compound (Chiralpak IC 30/70 EtOH (0.1 formic acid)/heptane, 1.0 mL/min, t_R = 12.1 min). LCMS (ES$^+$) 391 (M + H)$^+$, t_R = 3.47 min

(analytical method 1). ^{1}H NMR δ (ppm) (DMSO-d_6): 10.61 (1 H, s), 8.72 (1 H, s), 7.70 (1 H, d, J = 7.9 Hz), 7.56 (1 H, s), 7.45 (1 H, d, J = 8.0 Hz), 7.35 (2 H, d, J = 7.6 Hz), 7.27 (2 H, t, J = 7.5 Hz), 7.19 (1 H, t, J = 7.2 Hz), 4.60 (2 H, s), 4.39 (2 H, q, J = 9.7 Hz), 3.24 (1 H, dd, J = 6.8, 5.4 Hz), 2.93 (1 H, dd, J = 9.7, 6.8 Hz), 2.30 (1 H, dd, J = 9.7, 5.4 Hz). HRMS (ESI) calcd for $C_{20}H_{17}F_3N_2O_3$ [M + H]$^+$ 391.1269, found 391.1267.

(1R,2R,3R)-N-Hydroxy-2-(4-(2-methyloxazol-5-yl)phenyl)-3-phenylcyclopropanecarboxamide (58). The synthesis involved following procedure A from **14i′** (460 mg). Purification by flash silica column chromatography (gradient elution DCM to 5% MeOH in DCM) and then preparative HPLC gave the racemic mixture as a white solid (35 mg, 59%). Preparative chiral HPLC gave the title compound (Chiralpak IC 40/60 EtOH (0.1% formic acid)/heptane, 1.0 mL/min, t_R = 12.0 min). LCMS (ES$^+$) 335 (M + H)$^+$. t_R = 3.28 min (analytical method 1). ^{1}H NMR δ (ppm) (DMSO-d_6): 10.50 (1 H, s), 8.63 (1 H, s), 7.55 (2 H, d, J = 8.1 Hz), 7.43 (1 H, s), 7.34–7.23 (4 H, m), 7.23–7.15 (2 H, m), 7.14–7.07 (1 H, m), 3.05 (1 H, dd, J = 6.8, 5.4 Hz), 2.81 (1 H, dd, J = 9.6, 6.8 Hz), 2.40 (3 H, s), 2.16 (1 H, dd, J = 9.6, 5.4 Hz). HRMS (ESI) calcd for $C_{20}H_{18}N_2O_3$ [M + H]$^+$ 335.1396, found 335.1391.

(1R,2R,3R)-2-(4-(2-Cyclopropyloxazol-5-yl)phenyl)-N-hydroxy-3-phenylcyclopropanecarboxamide (59). The synthesis involved following procedure A from compound **14k′** (300 mg, 0.80 mmol). Purification by flash silica column chromatography (gradient elution DCM to 3% MeOH in DCM) gave the racemic mixture as a white solid (300 mg, 78%). Preparative chiral HPLC gave the title compound (Chiralpak IC 30/70 EtOH (0.1 formic acid)/heptane, 1.0 mL/min, t_R = 19.8 min). LCMS (ES$^+$) 361 (M + H)$^+$, (ES$^-$) 359 (M − H)$^-$, t_R = 3.67 min (analytical method 1). ^{1}H NMR δ (ppm) (DMSO-d_6): 10.62 (1 H, s), 8.76 (1 H, s), 7.65 (2 H, d, J = 8.2 Hz), 7.52 (1 H, s), 7.42–7.35 (4 H, m), 7.31 (2 H, t, J = 7.5 Hz), 7.23 (1 H, t, J = 7.2 Hz), 3.17 (1 H, dd, J = 6.9, 5.4 Hz), 2.92 (1 H, dd, J = 9.7, 6.9 Hz), 2.28 (1 H, dd, J = 9.6, 5.4 Hz), 2.23–2.17 (1 H, m), 1.15–1.08 (2 H, m), 1.09–1.03 (2 H, m). HRMS (ESI) calcd for $C_{22}H_{20}N_2O_3$ [M + H]$^+$ 361.1552, found 361.1550.

(1R,2R,3R)-N-Hydroxy-2-(4-(oxazol-4-yl)phenyl)-3-phenyl-cyclopropanecarboxamide (60). The synthesis involved following procedure A from **14q′** (0.12 g, 0.37 mmol). Preparative chiral purification gave the title compound (Chiralpak IC 30/70 [IPA/MeOH (50/50/0.1% formic acid)]/heptane 5.0 mL/min, t_R = 11.47 min). LCMS (ES$^+$) 321 (M + H)$^+$, t_R = 9.76 min (analytical method 1). ^{1}H NMR δ (ppm) (DMSO-d_6): 10.56 (1 H, s), 8.69 (1 H, d, J = 1.8 Hz), 8.62 (1 H, s), 8.46 (1 H, d, J = 0.9 Hz), 7.76 (2 H, d, J = 8.1 Hz), 7.35 (4 H, d, J = 8.1 Hz), 7.30–7.24 (2 H, m), 7.20–7.15 (1 H, m), 3.12 (1 H, dd, J = 6.8, 5.4 Hz), 2.87 (1 H, dd, J = 9.5, 6.8 Hz), 2.24 (1 H, dd, J = 9.5, 5.4 Hz). HRMS (ESI) calcd for $C_{22}H_{20}N_2O_3$ [M + H]$^+$ 321.1239, found 321.1241.

(1R,2R,3R)-N-Hydroxy-2-(3-(oxazol-5-yl)phenyl)-3-phenyl-cyclopropanecarboxamide (61). The synthesis involved following procedure G from **7b** (500 mg, 1.45 mmol). Purification by flash silica column chromatography (gradient elution i-hex to 25% EtOAc in i-hex) gave (1R*,2R*,3R*)-ethyl 2-(3-(oxazol-5-yl)phenyl)-3-phenyl-cyclopropanecarboxylate (**9n**) as a colorless oil [494 mg, 100%, LCMS (ES$^+$) 334 (M + H)$^+$], which was progressed to the next step. The synthesis involved following procedure A from **9n** (482 mg, 1.45 mmol). Purification by flash silica column chromatography (gradient elution DCM to 5% MeOH in DCM) gave the racemic mixture as a white solid (233 mg, 50%). Preparative chiral HPLC gave the title compound (Chiralpak IC 40/60 EtOH (0.1 formic acid)/heptane, 1.0 mL/min, t_R = 7.7 min). LCMS (ES$^+$) 321 (M + H)$^+$, t_R = 2.82 min (analytical method 1). ^{1}H NMR δ (ppm) (DMSO-d_6): 10.62 (1 H, s), 8.76 (1 H, s), 8.52 (1 H, s), 7.80 (1 H, s), 7.70 (1 H, s), 7.64 (1 H, d, J = 7.8 Hz), 7.49 (1 H, t, J = 7.7 Hz), 7.42–7.28 (5 H, m), 7.24 (1 H, t, J = 7.2 Hz), 3.22 (1 H, dd, J = 6.9, 5.4 Hz), 2.98 (1 H, dd, J = 9.6, 6.9 Hz), 2.32 (1 H, dd, J = 9.6, 5.4 Hz). HRMS (ESI) calcd for $C_{19}H_{16}N_2O_3$ [M + H]$^+$ 321.1239, found 321.1241.

ASSOCIATED CONTENT

S Supporting Information

Modeling, crystallographic method, data collection and refinement statistics, synthesis of intermediates, biological activity methods, procedures used for the in vitro ADME and in vivo studies as well as metabolism and PK studies. This material is available free of charge via the Internet at http://pubs.acs.org.

AUTHOR INFORMATION

Corresponding Author

*Phone: +1 310-342-5503. E-mail: Celia.Dominguez@CHDIFoundation.org.

Author Contributions

The manuscript was written through contributions of all authors. All authors have given approval to the final version of the manuscript.

Notes

The authors declare no competing financial interest.

‖K.A.L.: Consultant to CHDI.

ACKNOWLEDGMENTS

ABBREVIATIONS USED

ee, enantiomeric excess; iv, intravenous; po, per os (oral); rt, room temperature; AUCN, area under the curve normalized for dose level; SAR, structure−activity relationship; BOP, benzotriazole-1-yloxytris(dimethylamino)phosphonium hexafluorophosphate; DCM, dichloromethane; DIPEA, diisopropylethylamine; DMA, dimethylacetamide; DME, dimethoxyethane; DMF, dimethylformamide; DMSO, dimethylsulfoxide; ES$^+$, electrospray positive ionization; ES$^-$, electrospray negative ionization; Et$_2$O, diethyl ether; EtOAc, ethyl acetate; h, hour; HPLC, high performance liquid chromatography; i-hex, isohexane; LCMS, liquid chromatography mass spectrometry; LiHMDS, lithium bis(trimethylsilyl)amide; M, mass; MeCN, acetonitrile; MeOH, methanol; Pd$_2$(dba)$_3$, tris-(dibenzylideneacetone)dipalladium(0); Pd(dppf)Cl$_2$, [1,1′-bis-(diphenylphosphino)ferrocene]dichloropalladium(II); o-tol, ortho tolyl; t$_R$, retention time; SPE, solid phase extraction; THF, tetrahydrofuran; xantphos, 4,5-bis(diphenylphosphino)-9,9-dimethylxanthene

REFERENCES

(1) Choudhary, C.; Kumar, C.; Gnad, F.; Nielsen, M. L.; Rehman, M.; Walther, T. C.; Olsen, J. V.; Mann, M. Lysine acetylation targets protein complexes and co-regulates major cellular functions. *Science* **2009**, *325*, 834−840.
(2) Aka, J. A.; Kim, G. W.; Yang, X. J. K-acetylation and its enzymes: overview and new developments. *Handb. Exp. Pharmacol.* **2011**, *206*, 1−12.
(3) McKinsey, T. A. The biology and therapeutic implications of HDACs in the heart. *Handb. Exp. Pharmacol.* **2011**, *206*, 57−78.
(4) Grabiec, A. M.; Tak, P. P.; Reedquist, K. A. Function of histone deacetylase inhibitors in inflammation. *Crit. Rev. Immunol.* **2011**, *31*, 233−263.
(5) Haggarty, S. J.; Tsai, L. H. Probing the role of HDACs and mechanisms of chromatin-mediated neuroplasticity. *Neurobiol. Learn. Mem.* **2011**, *96*, 41−52.

(6) Fischle, W.; Dequiedt, F.; Hendzel, M. J.; Guenther, M. G.; Lazar, M. A.; Voelter, W.; Verdin, E. Enzymatic activity associated with class II HDACs is dependent on a multiprotein complex containing HDAC3 and SMRT/N-CoR. *Mol. Cell* **2002**, *9*, 45−57.
(7) Yang, X. J.; Gregoire, S. Class II histone deacetylases: from sequence to function, regulation, and clinical implication. *Mol. Cell. Biol.* **2005**, *25*, 2873−2884.
(8) Verdin, E.; Dequiedt, F.; Kasler, H. G. Class II histone deacetylases: versatile regulators. *Trends Genet.* **2003**, *19*, 286−293.
(9) Clocchiatti, A.; Florean, C.; Brancolini, C. Class IIa HDACs: from important roles in differentiation to possible implications in tumourigenesis. *J. Cell. Mol. Med.* **2011**, *15*, 1833−1846.
(10) Lahm, A.; Paolini, C.; Pallaoro, M.; Nardi, M. C.; Jones, P.; Neddermann, P.; Sambucini, S.; Bottomley, M. J.; Lo Surdo, P.; Carfi, A.; Koch, U.; De Francesco, R.; Steinkuhler, C.; Gallinari, P. Unraveling the hidden catalytic activity of vertebrate class IIa histone deacetylases. *Proc. Natl. Acad. Sci. U.S.A.* **2007**, *104*, 17335−17340.
(11) Jones, P.; Altamura, S.; De Francesco, R.; Gallinari, P.; Lahm, A.; Neddermann, P.; Rowley, M.; Serafini, S.; Steinkuhler, C. Probing the elusive catalytic activity of vertebrate class IIa histone deacetylases. *Bioorg. Med. Chem. Lett.* **2008**, *18*, 1814−1819.
(12) Bradner, J. E.; West, N.; Grachan, M. L.; Greenberg, E. F.; Haggarty, S. J.; Warnow, T.; Mazitschek, R. Chemical phylogenetics of histone deacetylases. *Nat. Chem. Biol.* **2010**, *6*, 238−243.
(13) Fischle, W.; Kiermer, V.; Dequiedt, F.; Verdin, E. The emerging role of class II histone deacetylases. *Biochem. Cell Biol.* **2001**, *79*, 337−348.
(14) Mihaylova, M. M.; Vasquez, D. S.; Ravnskjaer, K.; Denechaud, P. D.; Yu, R. T.; Alvarez, J. G.; Downes, M.; Evans, R. M.; Montminy, M.; Shaw, R. J. Class IIa histone deacetylases are hormone-activated regulators of FOXO and mammalian glucose homeostasis. *Cell* **2011**, *145*, 607−621.
(15) Raichur, S.; Teh, S. H.; Ohwaki, K.; Gaur, V.; Long, Y. C.; Hargreaves, M.; McGee, S. L.; Kusunoki, J. Histone deacetylase 5 regulates glucose uptake and insulin action in muscle cells. *J. Mol. Endocrinol.* **2012**, *49*, 203−211.
(16) Ago, T.; Liu, T.; Zhai, P.; Chen, W.; Li, H.; Molkentin, J. D.; Vatner, S. F.; Sadoshima, J. A redox-dependent pathway for regulating class II HDACs and cardiac hypertrophy. *Cell* **2008**, *133*, 978−993.
(17) Ling, S.; Sun, Q.; Li, Y.; Zhang, L.; Zhang, P.; Wang, X.; Tian, C.; Li, Q.; Song, J.; Liu, H.; Kan, G.; Cao, H.; Huang, Z.; Nie, J.; Bai, Y.; Chen, S.; Li, Y.; He, F.; Zhang, L.; Li, Y. CKIP-1 inhibits cardiac hypertrophy by regulating class II histone deacetylase phosphorylation through recruiting PP2A. *Circulation* **2012**, *126*, 3028−3040.
(18) McKinsey, T. A.; Kuwahara, K.; Bezprozvannaya, S.; Olson, E. N. Class II histone deacetylases confer signal responsiveness to the ankyrin-repeat proteins ANKRA2 and RFXANK. *Mol. Biol. Cell* **2006**, *17*, 438−447.
(19) McKinsey, T. A.; Olson, E. N. Dual roles of histone deacetylases in the control of cardiac growth. *Novartis Found. Symp.* **2004**, *259*, 132−141 (discussion 141−145, 163−169).
(20) Kee, H. J.; Kook, H. Roles and targets of class I and IIa histone deacetylases in cardiac hypertrophy. *J. Biomed. Biotechnol.* **2011**, *2011*, 928326.
(21) Kong, Y.; Tannous, P.; Lu, G.; Berenji, K.; Rothermel, B. A.; Olson, E. N.; Hill, J. A. Suppression of class I and II histone deacetylases blunts pressure-overload cardiac hypertrophy. *Circulation* **2006**, *113*, 2579−2588.
(22) Matsushima, S.; Kuroda, J.; Ago, T.; Zhai, P.; Park, J. Y.; Xie, L. H.; Tian, B.; Sadoshima, J. Increased oxidative stress in the nucleus caused by Nox4 mediates oxidation of HDAC4 and cardiac hypertrophy. *Circ. Res.* **2013**, *112*, 651−663.
(23) Granger, A.; Abdullah, I.; Huebner, F.; Stout, A.; Wang, T.; Huebner, T.; Epstein, J. A.; Gruber, P. J. Histone deacetylase inhibition reduces myocardial ischemia−reperfusion injury in mice. *FASEB J.* **2008**, *22*, 3549−3560.
(24) Hancock, W. W.; Akimova, T.; Beier, U. H.; Liu, Y.; Wang, L. HDAC inhibitor therapy in autoimmunity and transplantation. *Ann. Rheum. Dis.* **2012**, *71* (Suppl. 2), i46−i54.

(25) de Zoeten, E. F.; Wang, L.; Sai, H.; Dillmann, W. H.; Hancock, W. W. Inhibition of HDAC9 increases T regulatory cell function and prevents colitis in mice. *Gastroenterology* **2010**, *138*, 583–594.

(26) Mannaerts, I.; Eysackers, N.; Onyema, O. O.; Van Beneden, K.; Valente, S.; Mai, A.; Odenthal, M.; van Grunsven, L. A. Class II HDAC inhibition hampers hepatic stellate cell activation by induction of MicroRNA-29. *PLoS One* **2013**, *8*, e55786.

(27) Mielcarek, M.; Benn, C. L.; Franklin, S. A.; Smith, D. L.; Woodman, B.; Marks, P. A.; Bates, G. P. SAHA decreases HDAC 2 and 4 levels in vivo and improves molecular phenotypes in the R6/2 mouse model of Huntington's disease. *PLoS One* **2011**, *6*, e27746.

(28) Mielcarek, M.; Landles, C.; Weiss, A.; Bradaia, A.; Seredenina, T.; Inuabasi, L.; Osborne, G. F.; Wadel, K.; Touller, C.; Butler, R.; Robertson, J.; Franklin, S. A.; Smith, D. L.; Park, L.; Marks, P. A.; Wanker, E. E.; Olson, E. N.; Luthi-Carter, R.; van der Putten, H.; Beaumont, V.; Bates, G. P. HDAC4 reduction: a novel therapeutic strategy to target cytoplasmic huntingtin and ameliorate neurodegeneration. *PLoS Biol.*, submitted.

(29) Sung, Y. M.; Lee, T.; Yoon, H.; DiBattista, A. M.; Song, J. M.; Sohn, Y.; Moffat, E. I.; Turner, R. S.; Jung, M.; Kim, J.; Hoe, H. S. Mercaptoacetamide-based class II HDAC inhibitor lowers Abeta levels and improves learning and memory in a mouse model of Alzheimer's disease. *Exp. Neurol.* **2013**, *239*, 192–201.

(30) Hobara, T.; Uchida, S.; Otsuki, K.; Matsubara, T.; Funato, H.; Matsuo, K.; Suetsugi, M.; Watanabe, Y. Altered gene expression of histone deacetylases in mood disorder patients. *J. Psychiatr. Res.* **2010**, *44*, 263–270.

(31) Iga, J.; Ueno, S.; Yamauchi, K.; Numata, S.; Kinouchi, S.; Tayoshi-Shibuya, S.; Song, H.; Ohmori, T. Altered HDAC5 and CREB mRNA expressions in the peripheral leukocytes of major depression. *Prog. Neuropsychopharmacol. Biol. Psychiatry* **2007**, *31*, 628–632.

(32) Renthal, W.; Maze, I.; Krishnan, V.; Covington, H. E., 3rd; Xiao, G.; Kumar, A.; Russo, S. J.; Graham, A.; Tsankova, N.; Kippin, T. E.; Kerstetter, K. A.; Neve, R. L.; Haggarty, S. J.; McKinsey, T. A.; Bassel-Duby, R.; Olson, E. N.; Nestler, E. J. Histone deacetylase 5 epigenetically controls behavioral adaptations to chronic emotional stimuli. *Neuron* **2007**, *56*, 517–529.

(33) Tsankova, N.; Renthal, W.; Kumar, A.; Nestler, E. J. Epigenetic regulation in psychiatric disorders. *Nat. Rev. Neurosci.* **2007**, *8*, 355–367.

(34) Tsankova, N. M.; Berton, O.; Renthal, W.; Kumar, A.; Neve, R. L.; Nestler, E. J. Sustained hippocampal chromatin regulation in a mouse model of depression and antidepressant action. *Nat. Neurosci.* **2006**, *9*, 519–525.

(35) Cohen, T. J.; Barrientos, T.; Hartman, Z. C.; Garvey, S. M.; Cox, G. A.; Yao, T. P. The deacetylase HDAC4 controls myocyte enhancing factor-2-dependent structural gene expression in response to neural activity. *FASEB J.* **2009**, *23*, 99–106.

(36) Simmons, B. J.; Cohen, T. J.; Bedlack, R.; Yao, T. P. HDACs in skeletal muscle remodeling and neuromuscular disease. *Handb. Exp. Pharmacol.* **2011**, *206*, 79–101.

(37) Chen, J. F.; Mandel, E. M.; Thomson, J. M.; Wu, Q.; Callis, T. E.; Hammond, S. M.; Conlon, F. L.; Wang, D. Z. The role of microRNA-1 and microRNA-133 in skeletal muscle proliferation and differentiation. *Nat. Genet.* **2006**, *38*, 228–233.

(38) Williams, A. H.; Valdez, G.; Moresi, V.; Qi, X.; McAnally, J.; Elliott, J. L.; Bassel-Duby, R.; Sanes, J. R.; Olson, E. N. MicroRNA-206 delays ALS progression and promotes regeneration of neuromuscular synapses in mice. *Science* **2009**, *326*, 1549–1554.

(39) Choi, M. C.; Cohen, T. J.; Barrientos, T.; Wang, B.; Li, M.; Simmons, B. J.; Yang, J. S.; Cox, G. A.; Zhao, Y.; Yao, T. P. A direct HDAC4-MAP kinase crosstalk activates muscle atrophy program. *Mol. Cell* **2012**, *47*, 122–132.

(40) Hebach, C.; Kallen, J.; Nozulak, J.; Tintelnot-Blomley, M.; Widler, L. Novel Trifluoromethyl-oxadiazole Derivatives and Their Use in the Treatment of Disease. WO 2013/080120, June 6, 2013.

(41) Beconi, M.; Aziz, O.; Matthews, K.; Moumne, L.; O'Connell, C.; Yates, D.; Clifton, S.; Pett, H.; Vann, J.; Crowley, L.; Haughan, A. F.; Smith, D. L.; Woodman, B.; Bates, G. P.; Brookfield, F.; Burli, R. W.;

(42) Hoffmann, K.; Brosch, G.; Loidl, P.; Jung, M. A non-isotopic assay for histone deacetylase activity. *Nucleic Acids Res.* **1999**, *27*, 2057–2058.

(43) Ciossek, T.; Julius, H.; Wieland, H.; Maier, T.; Beckers, T. A homogeneous cellular histone deacetylase assay suitable for compound profiling and robotic screening. *Anal. Biochem.* **2008**, *372*, 72–81.

(44) Riester, D.; Wegener, D.; Hildmann, C.; Schwienhorst, A. Members of the histone deacetylase superfamily differ in substrate specificity towards small synthetic substrates. *Biochem. Biophys. Res. Commun.* **2004**, *324*, 1116–1123.

(45) Bottomley, M. J.; Lo Surdo, P.; Di Giovine, P.; Cirillo, A.; Scarpelli, R.; Ferrigno, F.; Jones, P.; Neddermann, P.; De Francesco, R.; Steinkuhler, C.; Gallinari, P.; Carfi, A. Structural and functional analysis of the human HDAC4 catalytic domain reveals a regulatory structural zinc-binding domain. *J. Biol. Chem.* **2008**, *283*, 26694–26704.

(46) Jones, P.; Bottomley, M. J.; Carfi, A.; Cecchetti, O.; Ferrigno, F.; Lo Surdo, P.; Ontoria, J. M.; Rowley, M.; Scarpelli, R.; Schultz-Fademrecht, C.; Steinkuhler, C. 2-Trifluoroacetylthiophenes, a novel series of potent and selective class II histone deacetylase inhibitors. *Bioorg. Med. Chem. Lett.* **2008**, *18* (141–145), 163–169.

(47) Muraglia, E.; Altamura, S.; Branca, D.; Cecchetti, O.; Ferrigno, F.; Orsale, M. V.; Palumbi, M. C.; Rowley, M.; Scarpelli, R.; Steinkuhler, C.; Jones, P. 2-Trifluoroacetylthiophene oxadiazoles as potent and selective class II human histone deacetylase inhibitors. *Bioorg. Med. Chem. Lett.* **2008**, *18*, 6083–6087.

(48) Tessier, P.; Smil, D. V.; Wahhab, A.; Leit, S.; Rahil, J.; Li, Z.; Deziel, R.; Besterman, J. M. Diphenylmethylene hydroxamic acids as selective class IIa histone deacetylase inhibitors. *Bioorg. Med. Chem. Lett.* **2009**, *19*, 5684–5688.

(49) Ontoria, J. M.; Altamura, S.; Di Marco, A.; Ferrigno, F.; Laufer, R.; Muraglia, E.; Palumbi, M. C.; Rowley, M.; Scarpelli, R.; Schultz-Fademrecht, C.; Serafini, S.; Steinkuhler, C.; Jones, P. Identification of novel, selective, and stable inhibitors of class II histone deacetylases. Validation studies of the inhibition of the enzymatic activity of HDAC4 by small molecules as a novel approach for cancer therapy. *J. Med. Chem.* **2009**, *52*, 6782–6789.

(50) Mai, A.; Massa, S.; Pezzi, R.; Simeoni, S.; Rotili, D.; Nebbioso, A.; Scognamiglio, A.; Altucci, L.; Loidl, P.; Brosch, G. Class II (IIa)-selective histone deacetylase inhibitors. 1. Synthesis and biological evaluation of novel (aryloxopropenyl)pyrrolyl hydroxyamides. *J. Med. Chem.* **2005**, *48*, 3344–3353.

(51) Mai, A.; Massa, S.; Pezzi, R.; Rotili, D.; Loidl, P.; Brosch, G. Discovery of (aryloxopropenyl)pyrrolyl hydroxyamides as selective inhibitors of class IIa histone deacetylase homologue HD1-A. *J. Med. Chem.* **2003**, *46*, 4826–4829.

(52) Lobera, M.; Madauss, K. P.; Pohlhaus, D. T.; Wright, Q. G.; Trocha, M.; Schmidt, D. R.; Baloglu, E.; Trump, R. P.; Head, M. S.; Hofmann, G. A.; Murray-Thompson, M.; Schwartz, B.; Chakravorty, S.; Wu, Z.; Mander, P. K.; Kruidenier, L.; Reid, R. A.; Burkhart, W.; Turunen, B. J.; Rong, J. X.; Wagner, C.; Moyer, M. B.; Wells, C.; Hong, X.; Moore, J. T.; Williams, J. D.; Soler, D.; Ghosh, S.; Nolan, M. A. Selective class IIa histone deacetylase inhibition via a nonchelating zinc-binding group. *Nat. Chem. Biol.* **2013**, *9*, 319–325.

(53) Verma, R. P. Hydroxamic acids as matrix metalloproteinase inhibitors. *EXS* **2012**, *103*, 137–176.

(54) Berman, H. M.; Westbrook, J.; Feng, Z.; Gilliland, G.; Bhat, T. N.; Weissig, H.; Shindyalov, I. N.; Bourne, P. E. The Protein Data Bank. *Nucleic Acids Res.* **2000**, *28*, 235–242.

(55) Vannini, A.; Volpari, C.; Gallinari, P.; Jones, P.; Mattu, M.; Carfi, A.; De Francesco, R.; Steinkuhler, C.; Di Marco, S. Substrate binding to histone deacetylases as shown by the crystal structure of the HDAC8-substrate complex. *EMBO Rep.* **2007**, *8*, 879–884.

(56) Bressi, J. C.; Jennings, A. J.; Skene, R.; Wu, Y.; Melkus, R.; De Jong, R.; O'Connell, S.; Grimshaw, C. E.; Navre, M.; Gangloff, A. R.

McAllister, G.; Dominguez, C.; Munoz-Sanjuan, I.; Beaumont, V. Oral administration of the pimelic diphenylamide HDAC inhibitor HDACi 4b is unsuitable for chronic inhibition of HDAC activity in the CNS in vivo. *PLoS One* **2012**, *7*, e44498.

Exploration of the HDAC2 foot pocket: synthesis and SAR of substituted *N*-(2-aminophenyl)benzamides. *Bioorg. Med. Chem. Lett.* **2010**, *20*, 3142−3145.

(57) Schuetz, A.; Min, J.; Allali-Hassani, A.; Schapira, M.; Shuen, M.; Loppnau, P.; Mazitschek, R.; Kwiatkowski, N. P.; Lewis, T. A.; Maglathin, R. L.; McLean, T. H.; Bochkarev, A.; Plotnikov, A. N.; Vedadi, M.; Arrowsmith, C. H. Human HDAC7 harbors a class IIa histone deacetylase-specific zinc binding motif and cryptic deacetylase activity. *J. Biol. Chem.* **2008**, *283*, 11355−11363.

(58) Dowling, D. P.; Gantt, S. L.; Gattis, S. G.; Fierke, C. A.; Christianson, D. W. Structural studies of human histone deacetylase 8 and its site-specific variants complexed with substrate and inhibitors. *Biochemistry* **2008**, *47*, 13554−13563.

(59) Corey, E. J.; CHaykovsky, M. Dimethylsulfoxonium methylide. *J. Am. Chem. Soc.* **1962**, *84*, 867−868.

(60) Corey, E. J.; Chaykovsky, M. Dimethyloxosulfonium methylide $((CH_3)_2SOCH_2)$ and dimethylsulfonium methylide $((CH_3)_2SCH_2)$. Formation and application to organic synthesis. *J. Am. Chem. Soc.* **1965**, *87*, 1353−1364.

(61) Corey, E. J.; Jautelat, M. Construction of ring systems containing the gemdimethylcyclopropane unit using diphenylsulfonium isopropylide. *J. Am. Chem. Soc.* **1967**, *89*, 3912−3914.

(62) Hopkins, A. L.; Groom, C. R.; Alex, A. Ligand efficiency: a useful metric for lead selection. *Drug Discovery Today* **2004**, *9*, 430−431.

(63) Leeson, P. D.; Springthorpe, B. The influence of drug-like concepts on decision-making in medicinal chemistry. *Nat. Rev. Drug Discovery* **2007**, *6*, 881−890.

(64) Wu, H.; Du, L. M. Spectrophotometric determination of anilines based on charge-transfer reaction. *Spectrochim. Acta, Part A* **2007**, *67*, 976−979.

(65) Mulder, G. J.; Meerman, J. H. Sulfation and glucuronidation as competing pathways in the metabolism of hydroxamic acids: the role of N,O-sulfonation in chemical carcinogenesis of aromatic amines. *Environ. Health Perspect.* **1983**, *49*, 27−32.

(66) Obach, R. S. Potent inhibition of human liver aldehyde oxidase by raloxifene. *Drug Metab. Dispos.* **2004**, *32*, 89−97.

(67) Tang, H.; Macpherson, P.; Marvin, M.; Meadows, E.; Klein, W. H.; Yang, X. J.; Goldman, D. A histone deacetylase 4/myogenin positive feedback loop coordinates denervation-dependent gene induction and suppression. *Mol. Biol. Cell* **2009**, *20*, 1120−1131.

(68) Sivaguru, J.; Sunoj, R. B.; Wada, T.; Origane, Y.; Inoue, Y.; Ramamurthy, V. Enhanced diastereoselectivity via confinement: diastereoselective photoisomerization of 2,3-diphenyl-1-benzoylcyclopropane derivatives within zeolites. *J. Org. Chem.* **2004**, *69*, 5528−5536.

(69) Martin, S. F.; Austin, R. E.; Oalmann, C. J.; Baker, W. R.; Condon, S. L.; deLara, E.; Rosenberg, S. H.; Spina, K. P.; Stein, H. H.; Cohen, J.; et al. 1,2,3-Trisubstituted cyclopropanes as conformationally restricted peptide isosteres: application to the design and synthesis of novel renin inhibitors. *J. Med. Chem.* **1992**, *35*, 1710−1721.

(70) Doyle, M. P.; Loh, K.-L.; DeVries, K. M.; Chinn, M. S. Enhancement of stereoselectivity in catalytic cyclopropanation reactions. *Tetrahedron Lett.* **1987**, *28*, 833−836.

■ NOTE ADDED AFTER ASAP PUBLICATION

This paper was published ASAP on December 5, 2013, with incorrect structures for compounds **56** and **57** in Table 7. The corrected version was reposted on December 12, 2013.